New tools for carbohydrate sulphation analysis: Heparan Sulphate 2-*O*-sulphotransferase (HS2ST) is a target for small molecule protein kinase inhibitors

Dominic P Byrne*, Yong Li*, Krithika Ramakrishnan*, Igor L Barsukov*, Edwin A Yates*, Claire E Eyers*§, Dulcé Papy-Garcia†, Sandrine Chantepie†, Vijayakanth Pagadala[#], Jian Liu+, Carrow Wells^, David H Drewry^, William J Zuercher^¶, Neil G Berry‡, David G Fernig* and Patrick A Eyers*||

* Department of Biochemistry, Institute of Integrative Biology, University of Liverpool, L69 7ZB, UK.

§ Centre for Proteome Research, Institute of Integrative Biology, University of Liverpool, L69 7ZB, UK.

† Laboratory CRRET CNRS 9215, Université Paris-Est, CRRET (EA 4397/ERL CNRS 9215), UPEC, F-94010, Créteil, France.

[#] Glycan Therapeutics, 617 Hutton Street, Raleigh, NC 27606, USA.

+ UNC Eshelman School of Pharmacy, University of North Carolina at Chapel Hill, Chapel Hill, NC, 27599, USA.

^ Structural Genomics Consortium, UNC Eshelman School of Pharmacy, University of North Carolina at Chapel Hill, Chapel Hill, NC, 27599, USA.

¶ Lineberger Comprehensive Cancer Center, University of North Carolina at Chapel Hill, Chapel Hill, NC 27599, USA.

‡ Department of Chemistry, University of Liverpool, L69 7ZD, UK

|| Correspondence to Patrick.eyers@liverpool.ac.uk

ABSTRACT:

Sulphation of carbohydrate residues occurs on a variety of glycans destined for secretion, and this modification is essential for efficient matrix-based signal transduction. Heparan sulphate (HS) glycosaminoglycans control physiological functions ranging from blood coagulation to cell proliferation. HS biosynthesis involves membrane-bound Golgi sulphotransferases, including heparan sulphate 2-*O*-sulphotransferase (HS2ST), which transfers sulphate from the co-factor PAPS (3'-phosphoadenosine 5'-phosphosulphate) to the 2-*O* position of α-L-iduronate in the maturing polysaccharide chain. The current lack of simple non-radioactive enzyme assays that can be used to quantify the levels of carbohydrate sulphation hampers kinetic analysis of this process and the discovery of HS2ST inhibitors. In this paper, we describe a new procedure for thermal shift analysis of purified HS2ST. Using this approach, we quantify HS2ST-catalyzed oligosaccharide sulphation using a novel synthetic fluorescent substrate and screen the Published Kinase Inhibitor Set (PKIS), to evaluate compounds that inhibit catalysis. We report the susceptibility of HS2ST to a variety of cell permeable compounds *in vitro*, including polyanionic polar molecules, the protein kinase inhibitor rottlerin and oxindole-based RAF kinase inhibitors. In a related study, published back-to-back with this article, we demonstrate that Tyrosyl Protein Sulpho Tranferases (TPSTs) are also inhibited by a variety of protein kinase inhibitors. We propose that appropriately validated small molecule compounds could become new tools for rapid inhibition of glycan (and protein) sulphation in cells, and that protein kinase inhibitors might be repurposed or redesigned for the specific inhibition of HS2ST.

SHORT TITLE: Inhibition of HS2ST by protein kinase inhibitors

ABBREVIATIONS: DSF: Differential Scanning Fluorimetry; **GlcA:** β-D-glucouronate; **HS2ST**: heparan sulphate 2-*O*-sulphotransferase **IdoA:** α-L-iduronate; **PAPS:** (Adenosine 3′-phosphate 5′-phosphosulphate; **PKIS:** Published Kinase Inhibitor Set; **RAF:** Rapidly Accelerated Fibrosarcoma; **TSA:** Thermostability Assay

KEYWORDS: HS2ST, PAPS, glycan, substrate PAPS, screening, enzyme, kinase, inhibitor

SUMMARY STATEMENT: We report that HS2ST, which is a PAPS-dependent glycan sulphotransferase, can be assayed using a variety of novel biochemical procedures, including a non-radioactive enzyme-based assay that detects glycan substrate sulphation in real time. HS2ST activity can be inhibited by different classes of compounds, including known protein kinase inhibitors, suggesting new approaches to evaluate the roles of HS2ST-dependent sulphation with small molecules in cells.

WORD COUNT INCLUDING REFERENCES: 11,087

INTRODUCTION:

Biological sulphation is a widespread reversible covalent modification found throughout nature [1]. The regulated sulphation of saccharides is critical for cellular signalling, including regulatory interactions between extracellular glycoproteins that control signal transduction and high-affinity interactions between different cellular surfaces [2]. In addition to providing mechanical strength, the sulphate-rich extracellular matrix also represents a hub for sulphation-based communication through growth factor signalling [3]. For example, FGF-receptor interactions and intracellular signaling to the ERK pathway are blunted in the absence of appropriate 2-*O* sulphation driven by heparan sulphate (HS)-modifying enzymes [4-9], while sulphation of the tetrasaccharide Sialyl Lewis^X antigen on glycolipids controls leukocyte adhesion to the endothelium during inflammation [10, 11]. Inappropriate glycan sulphation can therefore underlie aspects of abnormal signalling, infection, inflammation and, increasingly, human neuropathies [12], suggesting that targeting of carbohydrate sulphation dynamics using small molecule enzyme inhibitors may be of value in both basic and translational research [13]. Indeed, the current limited chemical toolbox to rapidly modify and study glycan sulphation is based around small molecule inhibitors of sulphatase-2 (Sulf-2), such as OKN-007 [14] or heparanase inhibitors and HS mimics, including roneparstat and PG545, which have been employed for basic and clinical investigation [15].

Glycan sulphotransferases (STs) can be classified into several families depending upon the positional substrate specificity of enzymes for their respective sugar substrates [16, 17]. Heparan sulphate 2-*O*-sulphotransferase (HS2ST) is required for the generation of HS, which is an abundant unbranched extracellular glycosaminoglycan with key roles in a range of physiological functions, most notably growth-factor dependent signalling related to development, cell migration and inflammation [18]. HS2ST is a transmembrane protein whose catalytic domain faces into the lumen of the Golgi compartment, and catalyses the sulphation of iduronic acid and, to a lesser extent β-D-glucouronate (GlcA), during the enzymatic assembly of secretory HS proteoglycans [18, 19]. HS2ST transfers the sulpho-moiety from PAPS (3'-phosphoadenosine 5'-phosphosulphate) sulphate donor to the C2 hydroxyl of IdoA that lies adjacent to an *N*-sulphated glucosamine residue, generating a 2-*O*-sulphated saccharide unit [20-22]. Removal of the sulphate by endosulphatases such as Sulf-2, or more general HS processing by heparanase, also contributes to the complex physiological patterns of carbohydrate editing found *in vivo* [23].

The analysis of murine models lacking HS2ST reveals central roles for 2-*O*-sulphated HS in kidney development and neuronal function, and for signalling through WNT and FGF-dependent pathways [8, 18, 24-26]. However, in order to carefully control and examine the dynamics and structural heterogeneity of 2-*O* sulphation patterns in HS, which are the consequences of nontemplate-based synthesis of HS and complex dynamic sulphation patterns, new small molecule approaches for the

direct, reversible, inhibition of sulphotransferase enzymes are urgently required. In particular, these need to be deployed using chemical biology strategies to overcome deficiencies associated with genetic disruption approaches relevant to development and/or compensatory glycosylation or signalling mechanisms [27].

Mechanistic parallels between the enzymatic pathway of biological sulphation by sulphotransferases [28] and phosphorylation by protein kinases [29] are apparent, since both enzyme classes transfer charged chemical units from an adenine-based nucleotide co-factor to a (usually) polymeric acceptor structure. The biological analysis of protein kinases, which are thought to employ a similar 'in-line' enzyme reaction as the 2-*O* sulphotransferases [28] when transferring phosphate to peptide targets [30], has been revolutionised by the synthesis and wide availability of small molecule inhibitors [31]. Many of these compounds were originally discovered in screens with ATP-competitive inhibitor libraries using oncology-associated target enzymes [32]. Protein kinases have proven to be exceptional targets for the development of therapeutic agents in humans, and ~50 kinase inhibitors have been approved, or will soon be approved, for cancer and anti-inflammatory indications [33]. To help diversify and accelerate this process, validated open-source panels of such inhibitors, such as the Public Kinase Inhibitor Set (PKIS), have been assembled for screening purposes, constituting a variety of chemotypes for unbiased small molecule inhibitor discovery, which can be applied to a diverse range of protein targets [34].

The analysis of carbohydrate sulphation currently relies heavily on genetic, biophysical (NMR) and combinatorial organic chemistry and enzymatic analysis, with only a handful of low-affinity inhibitors of carbohydrate sulphotransferases ever having been disclosed [13, 35]. More recently, a relatively potent inhibitor of the related Type IV aryl sulphotransferase [36] and much lower affinity oestrogen sulphotransferases inhibitors [37-39] were reported. Due to a lack of any selective chemical tool compounds, cellular glycan sulphation remains understudied, relying on non-specific cellular methods such as chlorate exposure [40], and the field remains ripe for technological innovation and new chemical biology approaches. Early attempts to discover such molecules amongst small, relatively unfocussed, kinase-based libraries led to the discovery of low-affinity purine and tyrphostin-based inhibitory compounds, which are well-established chemical classes of protein kinase inhibitor [35]. This raises the question as to whether PAPS-dependent sulphotransferases are general inhibitory targets for new or repurposed small molecules that target nucleotide-binding sites, especially broader families of compounds originally developed as protein kinase inhibitors. However, the low throughput nature of radioactive (^{35}S-PAPS) TLC or HPLC-based assays typically used for sulphotransferase analysis [35, 41, 42], and the relatively low potency of current hits, argues for new approaches to assay and screen more diverse selections of focused or larger chemical libraries.

In this paper, and in a related study employing tyrosyl protein sulphotranserases [Byrne et al.,

126 Biochemical Journal, *In Press*], we describe novel *in vitro* methods for assaying recombinant HS2ST,
127 one of which employs a fluorescent-based detection system with a hexasaccharide substrate. PAPS-
128 dependent sulphation of the substrate at the 2-*O* position of the IdoA residue leads to a change in
129 substrate chemical properties, which can be detected as a real-time mobility shift in a high-throughput
130 microfluidic assay format originally developed for the analysis of peptide phosphorylation [43, 44].
131 We exploit this assay alongside differential scanning fluorimetry (DSF) to screen a small molecule
132 PKIS library, characterising HS2ST susceptibility towards a variety of cell-permeable compounds.
133 We propose that appropriately validated small molecule ligands might become invaluable probes for
134 rapid cellular inhibition of HS2STs, and that further iteration could lead to the discovery, synthesis (or
135 repurposing) of small molecules, including compound classes currently employed as kinase inhibitors,
136 to probe cellular HS2ST function.

137

138

EXPERIMENTAL:

MATERIALS AND METHODS:

Chemicals and Compounds

Porcine intestinal heparin was from Sigma, oligomeric saccharide standards, termed dp2-dp12, where dp = degree of polymerisation [45], were from Iduron (Manchester, UK). Polymeric sulphated heparin-derivatives (Table 1) were synthesised in-house as previously described [46]. *N*-sulphated, fluorescein-tagged hexasaccharide glycan substrate (GlcNS-GlcA-GlcNS-IdoA-GlcNS-GlcA-fluorescein, where S=sulphation) containing either L-IdoA or GlcA residues at the third residue from the reducing end (to which a linker and the fluorophore were conjugated) were both purchased from GLYCAN therapeutics (Chapel Hill, NC). All standard laboratory biochemicals, were purchased from either Melford or Sigma, and were of the highest analytical quality. PAPS (adenosine 3'-phosphate 5'-phosphosulphate, lithium salt hydrate, APS (adenosine 5'-phosphosulphate, sodium salt), PAP (adenosine 3'-5'-diphosphate, disodium salt), CoA (coenzymeA, sodium salt) dephosphoCoA (3'-dephosphoCoA, sodium salt hydrate), ATP (adenosine 5'-triphosphate, disodium salt hydrate) ADP (adenosine 5'-diphosphate, disodium salt), AMP (adenosine 5'-monophosphate, sodium salt), GTP (guanosine 5'-triphosphate, sodium salt hydrate), or cAMP (adenosine 3',5'-cyclic monophosphate, sodium salt) were all purchased from Sigma and stored at -80°C to minimise degradation. Rottlerin, suramin, aurintricarboxylic acid and all named kinase inhibitors were purchased from Sigma, BD laboratories, Selleck or Tocris.

Cloning, recombinant protein production and SDS-PAGE

Chicken HS2ST (isoform 1), which exhibits ~92% identity to human HS2ST, was a kind gift from Dr Lars Pedersen (NIH, USA), and was expressed in the Rosetta-gami (DE3) strain of *E. coli* from a modified pMAL-c2x plasmid encoding an N-terminal maltose-binding protein (MBP) affinity tag. Trimeric recombinant HS2ST1 enzyme was partially purified using immobilised amylose affinity chromatography directly from the cleared bacterial extract, essentially as described previously [28]. MBP-HS2ST was eluted with maltose and further purified by SEC using a HiLoad 16/600 Superdex 200 column (GE Healthcare), which was equilibrated in 50 mM Tris–Cl, pH 7.4, 100 mM NaCl, 10% (v/v) glycerol and 1 mM DTT. Prior to analysis, purified proteins were snap frozen in liquid nitrogen and stored at -80°C. This procedure generated HS2ST of >95% purity. Proteolytic removal of the MBP affinity tag from HS2ST (after re-cloning with MBP and 3C protease sites into the plasmid pOPINM) led to rapid HS2ST denaturation, based on rapid precipitation, so for the procedures described in this paper the MBP affinity tag was left intact. For SDS-PAGE, proteins were denatured in Laemmli sample buffer, heated at 95°C for 5 min and then analysed by SDS-PAGE with 10% (v/v) polyacrylamide gels. Gels were stained and destained using a standard Coomassie Brilliant Blue protocol. To generate catalytically-inactive MBP-HS2ST, the conserved catalytic His residue (His

142) was mutated to Ala using standard PCR procedures [47]. The mutant enzyme was purified as described above.

DSF-based fluorescent assays

Thermal shift /stability assays (TSAs) were performed using a StepOnePlus Real-Time PCR machine (Life Technologies) using SYPRO-Orange dye (Emission max. 570 nm, Invitrogen), with thermal ramping between 20-95°C in 0.3°C step intervals per data point to induce denaturation in the presence or absence of test biochemicals or small molecule inhibitors, as previously described [47]. HS2ST was assayed at a final concentration of 5 μM in 50 mM Tris–Cl (pH 7.4) and 100 mM NaCl. Final DMSO concentration in the presence or absence of the indicated concentrations of ligand was no higher than 4% (v/v). Normalized data were processed using the Boltzmann equation to generate sigmoidal denaturation curves, and average $T_m/\Delta T_m$ values were calculated as described using GraphPad Prism software [47].

Microfluidics-based sulphation assay

N-sulphated, fluorescein-tagged hexasaccharide glycan substrate (GlcNS-GlcA-GlcNS-IdoA-GlcNS-GlcA-fluorescein, where S=sulphation) containing either L-IdoA or D-GlcA residues at the third residue from the reducing end (to which a linker and the fluorophore were conjugated) were both purchased from GLYCAN therapeutics (www.glycantherapeutics.com). The fluorescein group attached to the reducing end of the glycan substrate possesses a maximal emission absorbance of ~525 nm, which can be detected by the EZ Reader *via* LED-induced fluorescence. Chemically-modified heparins were generated through a published procedure [46], whereas oligosaccharides from Iduron were generated enzymatically [4, 48]. Non-radioactive microfluidic mobility shift carbohydrate sulphation assays were optimised in solution with a 12-sipper chip coated with SR8 reagent and a Perkin Elmer EZ Reader II system [49] using EDTA-based separation buffer and real-time kinetic evaluation of substrate sulphation. Pressure and voltage settings were adjusted manually to afford optimal separation of the sulphated product and non-sulphated hexasaccharide substrate, with a sample (sip) volume of 20 nl, and total assay times appropriate for the experiment. Individual sulphation assays were assembled in a 384 well plate in a volume of 80 μl in the presence of the indicated concentration of PAPS or various test compounds, 50 mM HEPES (pH 7.4), 0.015% (v/v) Brij-35 and 5 mM $MgCl_2$ (unless specified otherwise). The degree of oligosaccharide sulphation was directly calculated using EZ Reader software by measuring the sulpho oligosaccharide:oligosaccharide ratio at each time-point. The activity of HS2ST enzymes in the presence of biochemicals and small molecule inhibitors was quantified in 'kinetic mode' by monitoring the amount of sulphated glycan generated over the assay time, relative to control assay with no additional inhibitor molecule (DMSO control). Data was normalized with respect to these

control assays, with sulphate incorporation into the substrate limited to ~20 % to prevent depletion of PAPS and substrate and to ensure assay linearity. K*m* and IC_{50} values were determined by non-linear regression analysis with GraphPad Prism software.

NMR-based oligosaccharide sulphation analysis

For NMR experiments, fluorescein-labelled hexasaccharide L-IdoA substrate and the HS2ST-catalysed sulphation product (10 μM) dissolved in 50 mM HEPES, pH 7.4, 5 mM $MgCl_2$ and 0.002% (v/v) Brij-35 were lyophilised overnight and re-dissolved in an equivalent amount of D_2O. NMR experiments were performed at 25°C on a Bruker Avance III 800 MHz spectrometers equipped with a TCI CryoProbe. 1D and 2D proton and TOCSY spectra (mixing time 80 ms) were measured using standard pulse sequences provided by the manufacturer. Spectra were processed and analysed using TopSpin 3.4 software (Bruker).

HPLC-based oligosaccharide sulphation analysis

The fluorescein-labelled hexasaccharide L-IdoA substrate and the HS2ST-catalysed sulphation product (10 μM) were analyzed after anion-exchange chromatography by HPLC as previously described [50]. Oligosaccharides were digested in the presence of a mixture of heparitinase I, II and III. Samples were loaded on a Proteomix SAX-NP5 (SEPAX) column and eluted with an NaCl gradient. Column effluent was mixed (1:1) with 2% (v/v) 2-cyanoacetamide in 250mM of NaOH and subsequently monitored with a fluorescence detector (JASCO; FP-1520) either at 346 nm excitation and 410 nm emission (detection of mono and disaccharides linked to cyanoacetamide) or at 490 nm excitation and 525 nm emission (for detection of trisaccharides linked to fluorescein).

Small molecule screening assays

The PKIS chemical library (Supplementary Figure 6, designated as SB, GSK or GW compound sets) comprises 367 largely ATP-competitive kinase inhibitors, covering 31 chemotypes originally designed to inhibit 24 distinct protein kinase targets [51]. Compounds were stored frozen as a 10 mM stock in DMSO. The library is characterised as highly drug-like (~70% with molecular weight <500 Da and clogP values <5). For initial screening, compounds dissolved in DMSO were pre-incubated with HS2ST for 10 minutes and then employed for DSF or sulphotransferase-based enzyme reactions, which were initiated by the addition of the universal sulphate donor PAPS. For inhibition assays, competition assays, or individual IC_{50} value determination, a compound range was prepared by serial dilution in DMSO, and added directly into the assay to the appropriate final concentration. All control experiments contained 4% (v/v) DMSO, which had essentially no effect on HS2ST activity. Individual chemicals and glycan derivatives were prepared and evaluated using NMR, HPLC, DSF or microfluidics-based assay protocols, as described above.

Docking studies

Docking models for rottlerin, suramin and GW407323A were built using Spartan16 (https://www.wavefun.com) and energy minimised using the Merck molecular forcefield. GOLD 5.2 (CCDC Software;) was used to dock molecules [52], with the binding site defined as 10 Å around the 5' phosphorous atom of PAP, using coordinates from chicken MBP-HS2ST PDB ID: 4NDZ [20]. A generic algorithm with ChemPLP as the fitness function [53] was used to generate 10 binding-modes per ligand in HS2ST. Protons were added to the protein. Default settings were retained for the "ligand flexibility" and "fitness and search options", however "GA settings" was changed to 200%.

RESULTS:

Analysis of human HS2ST ligand binding using a thermal stability assay (TSA)

To our knowledge, Differential Scanning Fluorimetry (DSF) has not previously been used to examine the thermal stability and thermal shift profiles of sulphotransferases in the presence or absence of biochemical ligands, such as those related to the sulphate donor PAPS (Figure 1A). We purified recombinant HS2ST catalytic domain (amino acids 69 to 356) fused to an *N*-terminal maltose-binding protein (MBP) tag to near homogeneity (Figure 1B) and evaluated its thermal denaturation profile with the MBP tag still attached in the presence of PAPS, heparin or maltose (Figure 1C). As a control, we examined the profile of maltose-binding protein (MBP) incubated with the same chemicals (Figure 1D). Unfolding of MBP-HS2ST in buffer generated a biphasic profile, and the upper region of this profile could be positively shifted (stabilised) by incubation with the HS2ST co-factor PAPS or the known HS2ST-interacting oligosaccharide ligand heparin (Figure 1C). In contrast, maltose incubation with MBP-HS2ST induced the same characteristic stabilisation profile observed when MBP was incubated with maltose and then analysed by DSF (Figure 1D). As expected, neither PAPS nor heparin induced stabilisation of MBP, confirming that effects on MBP-HS2ST were due to interaction with the sulphotransferase domain, rather than the affinity tag of the recombinant protein (Figure 1D, relevant ΔT_m values presented in Figure 1E). Consistently, PAPS did not stabilise the catalytic domain of the ATP-dependent catalytic subunit of cAMP-dependent protein kinase (PKAc), which instead binds with high affinity to the co-factor Mg-ATP [47], inducing a ΔT_m of >4°C (Figure 1F).

We next analysed the sensitivity of this assay for measuring HS2ST stability shifts over a wide range of PAPS concentrations, which confirmed dose-dependent stabilisation of recombinant HS2ST by PAPS, with detection of binding in the low micromolar range of the co-factor, equivalent to a molar ratio of ~1:1 HS2ST:PAPS (Supplementary Figure 1A). Subsequently, we explored the potential of this assay to detect binding of a putative IdoA-containing oligosaccharide substrate for HS2ST, confirming dose-dependent effects of this polymeric glycan over a range of concentrations, consistent with binding and conformational stability. Similar to PAPS, detection of binding was observed in the low micromolar range, equivalent to a molar ratio of ~1:1 HS2ST:glycan (Supplementary Figure 1B). We also evaluated binding of a panel of adenine-based cofactors (PAP and ATP), which suggested binding of divalent cation Mg^{2+} ions in an EDTA-sensitive manner (Supplementary Figure 1C), inducing a ΔTm of ~3°C, similar to that observed with the HS2ST co-factor PAPS. In contrast, removal of the sulpho moiety of PAPS, which creates the enzymatic end product PAP, did not abrogate HS2ST binding (Supplementary Figure 2A), consistent with structural analysis of the enzyme [28]. Neither PAP nor PAPS binding required Mg^{2+} ions, although the effect on stabilisation with Mg^{2+} ions was additive (Supplementary Figures 1C and 2A). The non-functional enzyme co-factor APS, in which the 3'-phosphate group of adenine is absent, did not induce HS2ST stabilisation,

confirming a requirement for this charged modification (Supplementary Figure 2A). We also established that CoA and acetyl CoA, which both contain a 3'-phosphoadenine moiety, clearly induced thermal stabilisation of HS2ST; loss of the 3'-phosphate group in dephospho CoA abolished this effect (Supplementary Figure 2A). Finally, we demonstrated that ATP, GTP and ADP, but not AMP or cAMP, were all effective at protecting HS2ST from thermal denaturation, suggesting that they are also HS2ST ligands (Supplementary Figure 2A).

Analysis of human HS2ST glycan binding using TSA

To extend our HS2ST thermal analysis to identify potential glycan substrates, we evaluated enzyme stability in the presence of synthetic glycan chains of different lengths and sulphation patterns (Table 1). Of particular interest for further assay development, thermal shift (stabilisation) was detected in this assay when hexasaccharide (dp6) or a higher degree of polymerisation oligosaccharide was incubated with the enzyme (Supplementary Figure 2B), suggesting that a dp6 glycan might represent the shortest potential partner suitable for HS2ST binding, a prerequisite for enzymatic modification. Interestingly, many of the chemically-modified heparins tested served as efficient HS2ST binding partners relative to the heparin control. The fully chemically sulphated $I_{2s,3s}A^{6s}{}_{3s}Ns$ hexamer induced a similar HS2ST stability-shift to heparin, whereas the singly and doubly desulphated hexamers induced slightly smaller stability shifts (Supplementary Figure 2C). Moreover, a putative $I_{2OH}A^{6OH}Ns$ substrate, which contains a 2-*O* moiety that is predicted to be the substrate for 2-*O*-sulphotransferases, also led to marked thermal stabilisation of HS2ST, suggestive of productive binding to HS2ST that might permit it to be sulphated in the presence of PAPS (Supplementary Figure 2C).

A novel microfluidic kinetic assay to directly measure oligosaccharide sulphation by HS2ST

In order to quantify the effects of various ligands on HS2ST enzyme activity, we sought to develop a new type of rapid non-radioactive solution assay that could discriminate the enzymatic incorporation of sulphate into a synthetic oligosaccharide substrate. Current protocols are time-consuming and cumbersome, requiring Mass Spectrometry, NMR or ^{35}S-based radiolabelling/HPLC separation procedures. Importantly, we next tested whether a version of a $I_{2OH}A^{6OH}NS$ containing a hexasaccharide substrate coupled to a linker and fluorescein at the reducing end, which interacts with HS2ST (Supplementary Figure 2C), could also be enzymatically sulphated by HS2ST using 'gold-standard' NMR-based sulphation detection [46]. The fluorescent $I_{2OH}A^{6OH}Ns$ could not be evaluated for binding to HS2ST by DSF, due to interference of the fluorescent group in the unfolding assay, which measures SYPRO-Orange fluorescence at a similar wavelength. Instead, to confirm sulphation of the fluorescein-labelled substrate, it was pre-incubated with PAPS and HS2ST to catalyse site-specific sulphation (Figure 2A). The NMR spectrum of the sulphated product compared to that of the non-modified substrate provided unequivocal evidence for sulphation at the 2-*O* position of the sugar, most notably due to the diagnostic shifts of anomeric H-1 and H-2 protons in the presence of the 2-*O*-

sulphate group linkage to the carbon atom (Figure 2B and Supplementary Figure 3). The 2-*O* sulphated IdoA hexameric product was also confirmed using an established HPLC-based approach [50], which demonstrated stoichiometric sulphation of an enzyme-derived substrate derivative (Supplementary Figure 4).

Next, we evaluated the incorporation of the sulphate moiety from PAPS into a fluorescently-labelled glycan substrate using a microfluidic assay that detects real-time changes in substrate covalent modification (notably the introduction of a negative charge) when an electric field is applied to the solution reaction. This ratiometric assay, which we and others have previously employed to detect the formal double negative charge induced by real-time peptide phosphorylation [43, 54-56], was able to detect real-time incorporation of sulphate into the oligosaccharide substrate, based on the different retention time of the product compared to the substrate (Figure 2C). No sulphated product was detected in the absence of HS2ST (Figure 2D), and prolonged incubation of substrate with HS2ST led to stoichiometric conversion of the substrate into the fully sulphated product (P), which migrated very differently to the substrate (S) 'marker' (Figure 2E). Analysis of product/(product + substrate) ratios of the peak heights allowed us to monitor sulphation over any appropriate assay time (Figures 2F), and the degree of sulphation could easily be varied as a function of PAPS concentration in the assay. Furthermore, no sulphated product was detected in the presence of buffer or PAPS alone (Figure 2F), allowing us to determine a K*m* value of ~1 μM for PAPS-mediated substrate hexasaccharide sulphation (Figure 2G). We also noted that high (>1 mM) concentrations of Mg^{2+} ions led to concentration-dependent increases in enzyme HS2ST activity (Figure 2H), consistent with the effects of Mg^{2+} ions identified in DSF assays (Supplementary Figure 2A). Next, we confirmed that sulphation was optimal when an appropriate modifiable IdoA substrate was present, with sulphation reduced by >90% when a GlcA residue was incorporated into the central disaccharide of the substrate instead (compare Supplementary Figures 5A and 5B). To further validate our assay, we evaluated a catalytically-inactive point mutant of HS2ST, in which the putative catalytic base (His 142) was mutated to Ala [28]. Purified H142A MBP-HS2ST appeared to be appropriately folded, and although it bound to PAPS and heparin (Supplementary Figure 6A-C), it was unable to efficiently catalyse sulphation of the fluorescent $I_{2OH}A^{6OH}NS$ hexasaccharide substrate, possessing < 1% of the activity observed with wild-type MBP-HS2ST (Supplementary Figure 6D).

Screening for small molecule inhibitors of HS2ST using DSF and microfluidic technology

The discovery of HS2ST inhibitors is hindered by a lack of a rapid and quantifiable assay for the facile detection of sulphate modification using a close mimic of a physiological substrate. Our discovery that a synthetic HS2ST glycan substrate could be readily sulphated and detected by enzymatic assay in solution, without the need for HPLC, NMR or radioactive procedures, meant that this approach might now be optimised for the discovery of small molecule HS2ST inhibitors. We first

evaluated the ability of an unlabelled (non-fluorescent) heparin glycan substrate that lacked sulphate at the 2-*O* position, or a non-substrate heparin that was fully sulphated at all potential sites, to act as HS2ST inhibitors in our fluorescent glycan sulphation assay. As detailed in Figure 3A, the fully sulphated glycan was a potent inhibitor, interfering with HS2ST-dependent sulphation of the substrate with an IC_{50} value of <10 nM, consistent with tight binding to the enzyme, as previously established using DSF (Supplementary Figure 2C). In contrast, a less highly sulphated substrate was still able to compete with the fluorescent substrate in a dose-dependent manner (fixed at 2 μM in this assay), as indicated by the IC_{50} value of <100 nM. We next compared the effects of PAP, ATP, CoA and dephospho-CoA, which all exhibit thermal stabilisation of HS2ST in DSF assays (Supplementary Figure 2A). Interestingly, PAP (IC_{50} ~2 μM), CoA (IC_{50} = 65 μM) and ATP (IC_{50} = 466 μM) were HS2ST inhibitors, whereas dephospho CoA (which lacks the 3'-phosphate moiety in CoA) was not (Figure 3B). Increasing the concentration of PAPS in the assay led to a decrease in the level of inhibition by both PAP and CoA (Figure 3C), suggesting a PAPS-competitive mode of inhibition, as predicted from the various shared chemical features of these molecules (Figure 1A).

Recent studies have demonstrated that PAPS-dependent tyrosyltransferases (TPSTs) are inhibited by non-nucleotide-based polyanionic chemicals [57]. However, to our knowledge, the inhibition of carbohydrate sulphotransferases by such compounds has not been reported. Using our microfluidic assay, we confirmed that the polysulphated compound suramin (an inhibitor of angiogenesis) and the polyaromatic polyanion aurintricarboxylate (an inhibitor of protein:nucleic acid interactions, DNA polymerase and topoisomerase II) demonstrated nanomolar inhibition of HS2ST, with IC_{50} values of 40 ± 1 nM and 123 ± 7 nM respectively (Figure 3D). In addition, the non-specific protein kinase inhibitor rottlerin also inhibited HS2ST with an IC_{50} of 6.4 μM. Increasing the concentration of PAPS in the sulphation assay decreased the inhibitory effect, consistent with a competitive mode of HS2ST inhibition for rottlerin (Figure 3E).

Protein kinase inhibitors are a new class of potential broad-spectrum HS2ST inhibitor

The finding that the non-specific kinase inhibitor rottlerin [58] was a micromolar inhibitor of HS2ST was of particular interest, especially given the remarkable progress in the development of kinase inhibitors as chemical probes, tool compounds and, latterly, clinically-approved drugs. Similarities between ATP and PAPS (Figure 1A), and the finding that ATP can both bind to, and inhibit, HS2ST activity (Supplementary Figure 2A and Figure 3B) raised the possibility that other ATP-competitive protein kinase inhibitors might also interact with HS2ST. In order to exploit our screening capabilities further, we established a 384-well assay to evaluate inhibition of PAPS-dependent glycan sulphation by HS2ST. The Published Kinase Inhibitor Set (PKIS) is a well-annotated collection of 367 high-quality ATP-competitive kinase inhibitor compounds that are ideal for compound repurposing or the discovery of new chemical ligands for orphan targets. We screened PKIS using DSF and enzyme-

based readouts (Figures 4A and B respectively). As shown in Figure 4A, when screened at 40 μM compound in the presence of 5 μM HS2ST, only a small percentage of compounds induced HS2ST stabilisation or destabilisation at levels similar to that seen with an ATP control. We focussed on compounds inducing HS2ST ΔT_m values between + 0.5°C and - 0.5°C, and re-screened each 'hit' compound using ratiometric HS2ST enzyme assays at a final compound concentration of 40 μM. We reported the enzyme activity remaining compared to DMSO, with rottlerin (IC_{50} = ~8 μM), suramin (IC_{50} = ~20 nM) and aurintricarboxylate (IC_{50} = ~90 nM) as positive controls (Figure 4B and Supplementary Figures 7 and 8). We also included the compound GW406108X in our enzyme assay, since it was structurally related to several 'hit' compounds from the DSF screen. As shown in Figure 4C, the three PKIS compounds with the highest inhibitory activity (red) exhibited IC_{50} values of between 20-30 μM towards HS2ST in the presence of 1 μM PAPS, similar to inhibition by rottlerin. Of particular interest, these three compounds were amongst the top ~10% of compounds in terms of their ΔT_m values (red spheres, Figure 4A). Chemical deconvolution of compounds revealed that all three were closely-related members of a class of oxindole-based RAF protein kinase inhibitor (Figure 4A). Subsequently, one other related indole RAF inhibitory compound from PKIS, GW305074, was also shown to be a mid-micromolar HS2ST inhibitor, whereas the related oxindole GW405841X (Supplementary Figure 8) did not inhibit HS2ST at any concentration tested (Figure 4C). Finally, we used combined DSF and enzyme assays to evaluate a broader panel of well-characterised kinase inhibitors (Supplementary Figure 9). Interestingly, neither the pan-kinase inhibitor staurosporine, nor several FDA-approved tyrosine kinase inhibitors caused thermal stabilisation of HS2ST at any concentration tested. Moreover, chemically diverse RAF inhibitors, including clinical RAF compounds such as dabrafenib and vemurafenib, were unable to inhibit HS2ST in our sensitive HS2ST enzyme, even at concentrations as high as 400 μM (Supplementary Figure 9B).

Docking analysis of HS2ST ligands

The X-Ray structure (PDB ID:4NDZ) of trimeric chicken MBP-HS2ST fusion protein bound to non-sulphated PAP (Adenosine-3'-5'-diphosphate, a potent HS2ST inhibitor that was identified in this study) and a polymeric oligosaccharide, have previously been reported [20, 28]. We employed a 3.45 Å structural dataset to dock rottlerin, suramin and the most potent oxindole-based 'hit' from the screen (GW407323A, see Figure 4B) into the extended enzyme active site. As shown in Figure 5A, HS2ST possesses substrate-binding features that accommodates an extended oligosaccharide that place it in close proximity to the desulphated PAP end-product, which substitutes for the endogenous PAPS co-factor during crystallisation. The 3'-phosphoadenine moiety of PAP also helps anchor the nucleotide in an appropriate position. A molecular docking protocol for PAP in HS2ST was developed that matched the crystallographic binding pose of PAP extremely well (RMSD 0.31 Å, Figure 5B). By comparing a crystallised ligand (ADP) with docked rottlerin, suramin and

GW407323A, we confirmed that compounds could be docked into the active site of HS2ST broadly corresponding to either the PAPS-binding region (rottlerin and GW407323A, Figures 5C and D) or bridging both the substrate and co-factor binding sites (suramin, Figure 5E). In these binding modes, compounds make a number of stabilising amino acid interactions that permit them to compete with PAPS or oligosaccharide substrate for binding to HS2ST (Figure 5C, residue numbering based on the HS2ST trimer). For example, rottlerin is predicted to form a hydrogen bond with the amide backbone of Thr 1290, GW407323A has multiple potential hydrogen bonding interactions with residues including Arg 1080, Asn 1112 and Ser 1172, whilst suramin is predicted to form hydrogen bonds with residues Asn 1091, Tyr 1094 and Arg 1288, allowing this highly elongated inhibitor to straddle separate regions of the active-site.

DISCUSSION:

In this paper, we report a simple method for the detection of enzyme-catalysed glycan sulphation using a model IdoA-containing hexasaccharide fused to a reducing-end fluorophore. The chemical similarity between ATP, a universal phosphate donor, and PAPS, a universal sulphate donor, led us to investigate whether enzymatic glycan sulphation could be detected using a high-throughput kinetic procedure previously validated for peptide phosphorylation by ATP-dependent protein kinases. We focussed our attention on HS2ST, which transfers sulphate from PAPS to the 2-*O* position of IdoA during heparan sulphate biosynthesis in the secretory pathway.

To facilitate rapid purification of recombinant HS2ST, the enzyme was expressed as an N-terminal MBP fusion protein, and we confirmed that it was folded, and could bind to a variety of known exogenous ligands including PAPS and PAP, the end product of the sulphotransferase reaction. Protein kinases are also known to bind to their end-product (ADP), and kinase structural analysis has long taken advantage of the stability of kinase and ATP analogues, or ADP-like complexes, for protein co-crystallisation. Similar co-crystallisation approaches revealed the structure of HS2ST, and related sulphotransferases, in complex with PAP and model saccharide substrates [20, 21], and our study extends these approaches, by revealing a competitive mode of HS2ST interaction with a variety of 3'-phosphoadenosine-containing nucleotides, including Coenzyme A (CoA). They also suggest that generalised docking of a 3'phosphoadenosine moiety is a feature of HS2ST that could be mimicked using other small molecule inhibitors. DSF-based thermal shift assays are ideal for the analysis of a variety of proteins and ligands, including growth factors [4, 59], protein kinase domains [44, 47, 56], pseudokinase domains [60, 61], BH3 [62] and bromodomain-containing proteins [63]. However, to our knowledge, this is the first report to demonstrate the utility of a DSF-based strategy for the analysis of any sulphotransferase.

Competitive HS2ST inhibition by biochemical ligands

By developing a new type of rapid, kinetic glycan sulphation assay, we confirmed that many HS2ST ligands also act as competitive inhibitors of PAPS-dependent oligosaccharide sulphation, setting the stage for a broader screening approach for the discovery of HS2ST inhibitors. Standard assays for carbohydrate sulphation utilise HPLC-based detection of ^{35}S-based substrate sulphation derived from ^{35}S-lablled PAPS, requiring enzymatic co-factor synthesis and time-consuming radioactive solid-phase chromatography procedures [20, 35, 41]. Whilst enzymatic deconvolution, MS and NMR-based procedures remain useful for mapping sulphation patterns in complex (sometimes unknown) glycan polymers, these procedures are very time-consuming and relatively expensive. In contrast, our finding that sulphation can be detected using a simple glycan mobility shift assay, and then quantified in real-time by comparing the ratio of a sulphated and non-sulphated substrate, is rapid, reproducible and relatively inexpensive. Our kinetic assay makes use of a commercial platform originally developed for

the analysis of peptide phosphorylation or peptide proteolysis, which allows for the inclusion of high concentrations of non-radioactive co-factors, substrates and ligands in assays [44]. Consequently, we were able to use this technology to derive a K*m* value for PAPS in our standard HS2ST assay of 1.0 μM (Figure 2G), slightly lower than the reported literature value of 18.5 μM for HS2ST using desulphated heparin as substrate [20], but similar to the reported literature value of ~4.3 μM for the PAPS-dependent GlcNAc-6-sulphotransferase NodH from *Rhizobium melitoli* [35] and 1.5 and 10 μM for human hormone iodotyrosine sulphotransferases and tissue-purified tyrosyl sulphotransferase [64, 65]. In the course of our studies, we developed several new reagents, including a hexameric fluorescent substrate in which the central IdoA residue was replaced by a GlcA residue (Supplementary Figure 5). Interestingly, a decreased rate of substrate modification was observed using this oligosaccharide substrate, consistent with the ability of HS2ST to sulphate either IdoA or GlcA [19], but with a marked preference for the former. Previous HPLC-based studies identified an N-sulpho group in the oligosaccharide substrate as a pre-requisite for catalysis, with subsequent preferential transfer of sulphate to the 2-*O* position of IdoA [20, 22, 28, 66]; these published observations are entirely consistent with our findings using a hexameric fluorescent substrate.

In the future, it might be possible to quantify other site-specific covalent modifications in complex glycans using fluorescent oligosaccharides that contain distinct sugar residues, and by employing mobility-dependent detection in the presence of a variety of enzymes. These could include 3-*O* and 6-*O* sulphotransferases [21] or structurally distinct glycan phosphotransferases, such as the protein-*O*-mannose kinase POMK/Sgk196 [67], which catalyses an essential phosphorylation step during biosynthesis of an α-dystroglycan substrate [68]. Using this general approach, the screening and comparative analysis of small molecule inhibitors of these distinct enzyme classes would be simplified considerably relative to current procedures.

HS2ST inhibition by known kinase inhibitors, including a family of known RAF inhibitors

Our finding that HS2ST was inhibited at sub-micromolar concentrations by the compounds suramin [69] and the DNA polymerase inhibitor aurintricarboxylic acid [70] was intriguing, and consistent with recent reports demonstrating inhibitory activity of these compounds towards TPSTs, which employ PAPS as a co-factor, but instead sulphate tyrosine residues in specific motifs embedded in a variety of proteins [57]. During the course of our studies screening a panel of kinase inhibitors, we found that the non-specific kinase compound rottlerin is a micromolar inhibitor of HS2ST *in vitro*, with inhibition dependent upon the concentration of PAPS in the assay, suggesting a competitive mode of interaction. Rottlerin (also known as mallotoxin) is a polyphenolic compound from *Mallotus philippensis*, and although originally identified as an inhibitor of PKC isozymes [71], possesses a wide variety of biological effects likely due to its non-specific inhibition of multiple protein kinases [58]. This lack of specificity prevents exploitation of rottlerin in cells as a specific probe, although our

finding that HS2ST is a target of this compound opens up the possibility that this, or other, protein kinase inhibitors might also possess inhibitory activity towards HS2ST, either due to an ability to target the PAPS or oligosaccharide-binding sites in the enzyme. To evaluate these possibilities further, we screened PKIS, a collection of drug-like molecules with broad inhibitory activity towards multiple protein kinases. Interestingly, only 3 compounds (<1% of the library) consistently showed marked inhibitory activity at 40 μM in our HS2ST enzyme assay (Figure 4A, B and C, red). Remarkably, all three compounds belonged to the same benzylidene-1H-inol-2-one (oxindole) chemical class, which were originally reported as potent ATP-dependent RAF kinase inhibitors that block the MAPK signalling pathway in cultured cells [72]. Retrospectively, of all the related chemotypes present in the PKIS library, we confirmed that GW305074X (but not GW405841X) was also a micromolar HS2ST inhibitor, consistent with the broad sensitivity of HS2ST to this optimised class of RAF inhibitor.

Although limited Structure Activity Relationships can be derived from our initial studies, these findings demonstrate that HS2ST inhibitors can be discovered, and that several of these inhibitors could be of broad interest to the sulphotransferase (and protein kinase) fields. An additional outcome of our work is that pharmaceutical companies might conduct more extensive high-throughput screens using much larger libraries of kinase inhibitors to identify distinct, and more potent, leads. Our study also validates previous observations from the turn of the century, in which carbohydrate inhibitors of NoDH sulphotransferase were reported from a low diversity kinase-directed library [35]. Surprisingly, this early breakthrough did not lead to the development of any glycan sulphotransferase tool compounds for cell-based analysis. However, our discovery that oxindole-based RAF inhibitors are also HS2ST inhibitors could provide new impetus for the design and synthesis of much more specific and potent HS2ST inhibitors from this class of RAF kinase inhibitor, especially if issues of specificity can be evaluated using mutagenic target-validation approaches previously validated for various protein kinases [73-75].

A requirement for rapid progress during this process will be structure-based analysis of HS2ST in the presence of compounds, in order to determine mechanism and mode(s) of interaction. Our initial docking studies suggest similar binding modes for both rottlerin and the oxindole-based ligand GW407323A (Figure 5), with the potential for cross-over between PAPS and substrate-binding sites present on the surface of HS2ST. It will be intriguing to explore these binding modes by structural analysis and guided mutational approaches [76], in order to evaluate potential drug-binding site residues in HS2ST and to tease apart requirements for enzyme inhibition. It will also be important to assess whether compounds identified as *in vitro* HS2ST inhibitors, including previously reported RAF inhibitors, can also interfere with HS sulphation and downstream signalling in cells. Interestingly, suramin is a potent anti-angiogenic compound, and is reported to have cellular effects on FGF signalling [77], whereas aurintricarboxylate has multiple cellular effects currently attributed to

550 nucleotide-dependent processes. Attempting to link some of these cellular phenotypes to the inhibition
551 of 2-*O* glycan sulphation is a worthy future experimental strategy, although success with PAPS-
552 competitive compounds is likely to depend on the concentration of PAPS in the Golgi network and
553 the relative rate of, minimally, 2-*O* sulphate turnover (sulphation versus desulphation) amongst
554 physiological HS2ST substrates.

555

CONCLUSION:

Our work raises the possibility that HS2ST inhibitors could be developed strategically following the successful blueprint laid down for protein kinase inhibitors in the previous decades. Dozens of sulphotransferases are found in vertebrate genomes, and the development of chemical biology approaches to rapidly inactivate Golgi membrane-bound sulphotransferases and induce targeted inhibition of sulphation has been stymied by a lack of tool compounds, whose exploitation has the opportunity to revolutionise cell biology when properly validated [78, 79]. We propose that if such compounds can be developed, perhaps through high-throughput screening and discovery of new inhibitors, or even *via* chemical manipulation of the leads reported in this study, then a new era in sulphation-based cell biology might be on the horizon. By generating tools to chemically control glycan sulphation modulated by HS2ST directly, inhibitor-based interrogation of sulphation-dependent enzymes could also have significant impact in many active areas of translational research.

ACKNOWLEDGEMENTS:

This work was funded by a BBSRC Tools and Resources Development Grant (BB/N021703/1) and a Royal Society Research Grant (to PAE), a European Commission FET-OPEN grant (ArrestAD no.737390) to DPG, SC, DGF EAY and PAE, North West Cancer Research (NWCR) grants CR1088 and CR1097 and a NWCR endowment (to DGF). VP is supported by NIH Small Business Innovation Research Contract HHSN261201500019C. The SGC is a registered charity (number 1097737) that receives funds from AbbVie, Bayer Pharma AG, Boehringer Ingelheim, Canada Foundation for Innovation, Eshelman Institute for Innovation, Genome Canada, Innovative Medicines Initiative (EU/EFPIA) [ULTRA-DD grant no. 115766], Janssen, Merck KGaA Darmstadt Germany, MSD, Novartis Pharma AG, Ontario Ministry of Economic Development and Innovation, Pfizer, São Paulo Research Foundation-FAPESP, Takeda, and The Wellcome Trust [106169/ZZ14/Z].

AUTHOR CONTRIBUTIONS

PAE obtained BBSRC grant funding with DGF and EAY. PAE, DPB, EAY, ILB, CEE, DPG, SC and NGB designed and executed the experiments. VP, JL, CW, DHD and WJZ provided critical reagents, compound libraries, protocols and critical advice. PAE wrote the paper with contributions and final approval from all of the co-authors.

585 **FIGURE LEGENDS:**

586 **Figure 1. Analysis of purified recombinant MBP-HS2ST protein.**

587 **(A)** Structures of PAPS and PAPS-related biochemicals. **(B)** Coomassie blue staining of recombinant
588 MBP-HS2ST1 protein. ~2 μg of purified enzyme was analysed after SDS-PAGE. **(C)** Thermal
589 denaturation profiles of MBP-HS2ST (5 μM) and thermal shift in the presence of 0.5 mM PAPS (red),
590 10 μM heparin (blue) or 5 mM maltose (green). Buffer control is shown in black dashed lines. **(D)**
591 Thermal denaturation profile of purified recombinant maltose binding protein (MBP). Experimental
592 conditions as for (C). **(E)** T_m values measured for 5 μM MBP (squares) or MBP-HS2ST fusion
593 protein (triangles) in the presence of 0.5 mM PAPS, 10 μM heparin or 5 mM maltose. ΔT_m values
594 were obtained by DSF and calculated by subtracting control T_m values (buffer, no ligand) from the
595 measured T_m. **(F)** ΔT_m values relative to buffer addition for recombinant PKAc (5 μM) measured in
596 the presence of 0.5 mM PAPS, 0.5 mM ATP or 0.5 mM ATP and 10 mM $MgCl_2$. Similar results were
597 seen in three independent experiments.
598
599 **Figure 2. Development of a novel microfluidic mobility shift assay to quantify HS2ST enzymatic**
600 **activity.**
601 **(A)** Schematic showing PAPS-dependent sulphate incorporation into the fluorescein-labelled
602 hexasaccharide IdoA substrate by HS2ST, with the concomitant generation of PAP. R=fluorescein.
603 **(B)** NMR analysis of the non-sulphated and sulphated hexasaccharides. The addition of a 2-O-
604 sulphate group to the iduronate (L-IdoA) residue of the fluorescent hexasaccharide results in a
605 significant chemical shift change, most notably to the anomeric proton (H-1) and that of H-2 attached
606 to the sulphated carbon atom of L-IdoA, in agreement with expected values from the literature [46]. ^1H
607 NMR spectrum of non-sulphated substrate (bottom spectrum, black) and sulphated product (upper
608 spectrum, red). Distinct L-IdoA protons (H-3 and H-4 of the spin system) were identified by TOCSY
609 and are shown vertically above their respective H-1 signals (for the non-sulphated substrate, right blue
610 boxed, and for the sulphated product, left blue boxed). The full carbohydrate proton spectra are shown
611 in Supplementary Figure 3. **(C, D)** Screen shots of EZ reader II raw data files, demonstrating that
612 HS2ST induces a rapid mobility change in the IdoA-containing fluorescent hexasaccharide.
613 Separation of the higher mobility, sulphated (product, P) from the lower mobility (substrate, S)
614 hexasaccharide occurs as a result of enzymatic substrate sulphation (left panels 180 s assay time, right
615 panels 240 s assay time), as demonstrated by omission of HS2ST from the assay (-HS2ST). Assays
616 were initially performed at 20°C using 90 nM of purified HS2ST, 2 μM fluorescein-labelled
617 hexasaccharide substrate and 500 μM PAPS. **(E)** Stoichiometric sulphate-labelling of IdoA-containing
618 fluorescein-labelled hexasaccharide. Reactions were performed with 0.6 μM HS2ST, 375 μM IdoA-
619 hexasaccharide substrate and 1 mM PAPS and incubated at room temperature for 48 h. The reaction
620 was spiked with an additional 0.5 mM (final concentration) of PAPS after 24 h of incubation. M =

non-sulphated marker substrate. A final hexasaccharide concentration of 2 μM was analysed by fluorescent sulphation mobility assay. **(F)** Analysis of time-dependent sulphate incorporation into 2 μM IdoA-containing fluorescein-conjugated hexasaccharide. Percentage sulphation was calculated from the ratio of substrate hexasaccharide to product (2-*O*-sulpho)-hexasaccharide at the indicated time points in the presence or absence of 20 nM HS2ST and 10 μM PAPS. **(G)** Calculation of K*m* [PAPS] value for HS2ST. PAPS concentration was varied in the presence of a fixed concentration of HS2ST (20 nM), and the degree of substrate sulphation calculated from a differential kinetic analysis, n=2 assayed in duplicate. **(H)** Duplicate HS2ST assays conducted in the presence of increasing concentrations of activating Mg^{2+} ions. Activity is presented in duplicate relative to buffer controls. Similar results were seen in several independent experiments.

Figure 3. Microfluidic sulphotransferase assay to measure inhibition of HS2ST activity *in vitro.* Assays were performed using 20 nM HS2ST and the extent of substrate sulphation was determined after 15 min incubation at room temperature, as described in the legend to Figure 2. Dose-response curves for inhibition of HS2ST activity by **(A)** modified heparin derivatives containing different sulphation patterns (assayed in the presence of 0.5 mM $MgCl_2$) or **(B)** nucleotides (assayed in the absence of $MgCl_2$). Assays contained HS2ST and 10 μM PAPS and the indicated concentration of inhibitory ligand or buffer. **(C)** Inhibition of HS2ST activity by fixed 10 μM PAP, 0.5 mM CoA or 0.5 mM dephospho-CoA in the presence of increasing concentration of PAPS. Inhibition is calculated as a function of no inhibitor for each concentration of PAPS in the absence of $MgCl_2$. **(D)** Evaluation of small molecule HS2ST inhibitory profiles in the presence of 10 μM PAPS. **(E)** Inhibition of HS2ST activity by 20 μM rottlerin in the presence of varied concentrations of PAPS, suggesting a competitive mode of inhibition. Similar results were seen in multiple experiments.

Figure 4. Mining the PKIS inhibitor library for HS2ST inhibitor compounds. (**A)** Evaluation of small molecule ligands in a high-throughput HS2ST DSF assay. HS2ST (5 μM) was screened in the presence or absence of 40 μM compound. The final concentration of DMSO in the assay was 4 % (v/v). ΔT_m values (positive and negative) were calculated by subtracting the control T_m value (DMSO alone) from the measured T_m value. Data shown on a scatter plot of the mean ΔT_m values from two independent DSF assays. **(B)** Enzymatic analysis of HS2ST inhibition by selected PKIS compounds. HS2ST (20 nM) was incubated with the indicated PKIS compound (40 μM) in the presence of 10 μM PAPS for 15 mins at room temperature. HS2ST sulphotransferase activity was assayed using the fluorescent hexasaccharide substrate and normalised to DMSO control (4% v/v). **(C)** Full dose-response curves for selected compounds. HS2ST (20 nM) was incubated with increasing concentration of inhibitor in the presence of 1 μM PAPS for 15 mins at 20°C. HS2ST activity calculated as above. Data from two independent experiments are combined. Similar results were seen in an independent experiment.

Figure 5. Molecular docking analysis of HS2ST with small molecule inhibitor compounds.
(A) Structural representation of the catalytic domain of chicken MBP-HS2ST crystallised with bound heptasaccharide and non-sulphated PAP co-factor (Protein rendered as a cartoon. Red – α helix, yellow – β sheet, green – loop. PAP (Adenosine-3'-5'-diphosphate) and heptasaccharide are rendered as coloured sticks. Grey – carbon, red, oxygen, blue – nitrogen, yellow – sulphur. Black dotted line indicates close proximity of glycan 2-OH group and PAP. **(B)** Structure of HS2ST with near identical crystallographic (carbons in cyan) and docking (carbons in purple) poses of PAP (Protein rendered as a cartoon. Red – α helix, yellow – β sheet, green – loop. PAP rendered as coloured sticks. Cyan/Grey/Purple – carbon, red, oxygen, blue – nitrogen, dark yellow – sulphur). Black dotted lines indicate hydrogen bonds. Molecular Docking of **(C)** rottlerin, **(D)** the indole RAF inhibitor GW407323A or **(E)** suramin into the HS2ST catalytic domain (Protein depicted as a cartoon. Red – α helix, yellow – β sheet, green – loop. Docked molecules coloured as sticks. Pink/Yellow/Salmon/Grey – carbon, red, oxygen, blue – nitrogen, dark yellow – sulphur, white – hydrogen). Black dotted lines indicate hydrogen bonds. Amino acid numbering corresponds to that of trimeric HS2ST.

Supplementary Figure 1. Thermal stability analysis of MBP-HS2ST.
Concentration-dependent thermal profiling of MBP-HS2ST in the presence of **(A)** PAPS or **(B)** the chemically-modified heparin-derivative $I_{2OH}A^{60H}N_S$ (compound 7, see Table 1). ΔT_m values were calculated by DSF as previously described. **(C)** TSA assay showing changes in MBP-HS2ST thermostability induced by PAP and ATP, and the effects of EDTA and Mg^{2+}. Thermal stability of HS2ST was measured as a function of compound binding by DSF. ΔT_m values of HS2ST protein (5 μM) incubated with 0.5 mM of the indicated nucleotide ± 10 mM $MgCl_2$ ± 10 mM EDTA are shown.

Supplementary Figure 2. MBP-HS2ST Nucleotide and polysaccharide analysis.
(A) TSA showing MBP-HS2ST binding of nucleotides by DSF. Thermal stability was measured as a function of nucleotide binding by DSF. ΔT_m values of HS2ST protein (5 μM) incubated with 0.5 mM of the indicated nucleotide ± 10 mM $MgCl_2$ are shown. DSF analysis showing thermal shift (stabilization) of 5 μM HS2ST in the presence of 10 μM size separated oligosaccharide fragments, dp (degree of polymerisation) equivalent to disaccharide (dp2), tetrasaccharide (dp4), hexasaccharide (dp6), octasaccharide (dp8), decasaccharide (dp10) or dodecasaccharide (dp12) **(B)** or chemically-modified heparin derivatives **(C)**. The minimal hexasaccharide binding substrate in (B) and the putative HS2ST substrate $I_{2OH}A^{6OH}Ns$ in (C) are both shown in red. ΔT_m values (calculated as previously described) are normalized relative to heparin. dp=degree of polymerisation.

Supplementary Figure 3. NMR spectra of sulphated and non-sulphated fluorescent polysaccharide substrate.

TOCSY spectra of the L-IdoA-containing hexameric fluorescein-labelled HS2ST substrate (top) and the 2-O-sulphated product (bottom) generated by incubation with HS2ST, including the full spectrum of all carbohydrate hydrogens detected. Selected spectral regions, including the diagnostic shift caused by 2-O-sulphation, are expanded in Figure 2B in the main text, and are highlighted here by black and red boxes respectively.

Supplementary Figure 4. HPLC analysis of sulphated and non-sulphated fluorescent polysaccharide substrate.

HPLC separation of cyanoacetamide or fluorescein-labelled saccharides obtained from heparitinase digestion of GlcNS-GlcA-GlcNS-IdoA-GlcNS-GlcA-Fluorescein HS2ST substrate. Elution profiles of digested polysaccharide after anion exchange chromatography are shown. The non-sulphated IdoA-containing hexameric substrate (eluting at ~34 min, top) and the 2-*O*-sulphated product (eluting at ~37 min, bottom) were confirmed by comparison of the different peaks in the fluorescence spectra (dashed lines), with the later eluting sulphated product highlighted in red. dIdoA refers to the double bond formed by β-elimination between C4 and C5 in the IdoA and 2-*O*-IdoA oligosaccharides.

Supplementary Figure 5. HS2ST glycan residue substrate-specificity analysis.

Efficient sulphation of a hexasaccharide substrate by HS2ST requires an L-IdoA residue at the appropriate position in the oligosaccharide. Direct microfluidic sulphotransferase assays demonstrating time-dependent sulphation of the fluorescein-tagged hexasaccharide substrate containing either **(A)** L-IdoA or **(B)** D-GlcA residue at the third residue from the fluorescein-conjugated (reducing) end. R=fluorescein. The IdoA or GlcA residues are indicated in red.

Supplementary Figure 6. Analysis of purified recombinant H142A MBP-HS2ST1.

(A) Coomassie blue staining of H142A MBP-HS2ST protein. 2 μg of the mutant enzyme was analysed after SDS-PAGE. **(B)** Thermal denaturation profiles for H142A MBP-HS2ST (5 μM) in the presence of 0.5 mM PAPS (red), 10 μM heparin (blue) or 5 mM maltose (green). Buffer control is shown by the black dashed line. **(C)** ΔT_m values for H142A MBP-HS2ST measured in the presence of 0.5 mM PAPS (red) or 10 μM heparin (blue). Values were obtained by DSF and calculated by subtracting control T_m values (buffer, no ligands) from the measured T_m values. N=2, assayed in triplicate. **(D)** Direct microfluidic kinetic sulphotransferase assay comparing PAPS-dependent sulphation of fluorescein-tagged L-IdoA hexasaccharide by either WT MBP-HS2ST (red circles) or H142A MBP-HS2ST (red squares).

Supplementary Figure 7. HS2ST enzymatic PKIS compound screen.

Inhibition of HS2ST catalytic activity by selected PKIS members. Data are presented as HS2ST activity relative to DMSO control, assayed in duplicate. The most notable 'hit' inhibitors from the oxindole chemical class are shaded in red.

Supplementary Figure 8. Chemical structures of HS2ST inhibitory ligands.

Chemical structures of suramin, rottlerin, aurintricarboxylic acid and selected PKIS compounds.

Supplementary Figure 9. Lack of HS2ST inhibition by various kinase inhibitors.

DSF screening (left panel) or enzyme-based inhibitor assay (right panel) evaluating staurosporine, FDA-approved kinase inhibitors and several chemically-distinct RAF kinase inhibitors.

Table 1.

Predominant substitution patterns of differentially-sulphated heparin derivatives described in this study.

Analogue	Predominant repeat	IdoUA-2	GlcN-6	GlcN-2	IdoUA-3	GlcN-3a
1 (Heparin)	$I_{2S}A^{6S}Ns$	SO_3^-	SO_3^-	SO_3^-	OH	OH
2	$I_{2S}A^{6S}NAc$	SO_3^-	SO_3^-	$COCH_3$	OH	OH
3	$I_{2OH}A^{6S}Ns$	OH	SO_3^-	SO_3^-	OH	OH
4	$I_{2S}A^{6OH}Ns$	SO_3^-	OH	SO_3^-	OH	OH
5	$I_{2OH}A^{6S}NAc$	OH	SO_3^-	$COCH_3$	OH	OH
6	$I_{2S}A^{6OH}NAc$	SO_3^-	OH	$COCH_3$	OH	OH
7	$I_{2OH}A^{6OH}Ns$	OH	OH	SO_3^-	OH	OH
8	$I_{2OH}A^{6OH}NAc$	OH	OH	$COCH_3$	OH	OH
9	$I_{2S,3S}A^{6S}{}_{3S}Ns$	SO_3^-	SO_3^-	SO_3^-	SO_3^-	SO_3^-

REFERENCES:

1. Leung, A.W., I. Backstrom, and M.B. Bally, *Sulfonation, an underexploited area: from skeletal development to infectious diseases and cancer.* Oncotarget, 2016. **7**(34): p. 55811-55827.
2. Bowman, K.G. and C.R. Bertozzi, *Carbohydrate sulfotransferases: mediators of extracellular communication.* Chemistry & biology, 1999. **6**(1): p. R9-R22.
3. Kreuger, J., et al., *Interactions between heparan sulfate and proteins: the concept of specificity.* The Journal of cell biology, 2006. **174**(3): p. 323-7.
4. Li, Y., et al., *Heparin binding preference and structures in the fibroblast growth factor family parallel their evolutionary diversification.* Open biology, 2016. **6**(3).
5. Tillo, M., et al., *2- and 6-O-sulfated proteoglycans have distinct and complementary roles in cranial axon guidance and motor neuron migration.* Development, 2016. **143**(11): p. 1907-13.
6. Chan, W.K., D.J. Price, and T. Pratt, *FGF8 morphogen gradients are differentially regulated by heparan sulphotransferases Hs2st and Hs6st1 in the developing brain.* Biology open, 2017. **6**(12): p. 1933-1942.
7. Clegg, J.M., et al., *Heparan sulfotransferases Hs6st1 and Hs2st keep Erk in check for mouse corpus callosum development.* The Journal of neuroscience : the official journal of the Society for Neuroscience, 2014. **34**(6): p. 2389-401.
8. Chan, W.K., et al., *2-O Heparan Sulfate Sulfation by Hs2st Is Required for Erk/Mapk Signalling Activation at the Mid-Gestational Mouse Telencephalic Midline.* PloS one, 2015. **10**(6): p. e0130147.
9. Kreuger, J., et al., *Sequence analysis of heparan sulfate epitopes with graded affinities for fibroblast growth factors 1 and 2.* The Journal of biological chemistry, 2001. **276**(33): p. 30744-52.
10. Rosen, S.D. and C.R. Bertozzi, *Two selectins converge on sulphate. Leukocyte adhesion.* Current biology : CB, 1996. **6**(3): p. 261-4.
11. Sanders, W.J., et al., *L-selectin-carbohydrate interactions: relevant modifications of the Lewis x trisaccharide.* Biochemistry, 1996. **35**(47): p. 14862-7.
12. Sepulveda-Diaz, J.E., et al., *HS3ST2 expression is critical for the abnormal phosphorylation of tau in Alzheimer's disease-related tau pathology.* Brain : a journal of neurology, 2015. **138**(Pt 5): p. 1339-54.
13. Armstrong, J.I. and C.R. Bertozzi, *Sulfotransferases as targets for therapeutic intervention.* Current opinion in drug discovery & development, 2000. **3**(5): p. 502-15.
14. Williams, S.J., *Sulfatase inhibitors: a patent review.* Expert opinion on therapeutic patents, 2013. **23**(1): p. 79-98.
15. Lanzi, C., N. Zaffaroni, and G. Cassinelli, *Targeting Heparan Sulfate Proteoglycans and their Modifying Enzymes to Enhance Anticancer Chemotherapy Efficacy and Overcome Drug Resistance.* Current medicinal chemistry, 2017. **24**(26): p. 2860-2886.
16. Chapman, E., et al., *Sulfotransferases: structure, mechanism, biological activity, inhibition, and synthetic utility.* Angewandte Chemie, 2004. **43**(27): p. 3526-48.
17. Kakuta, Y., et al., *Conserved structural motifs in the sulfotransferase family.* Trends in biochemical sciences, 1998. **23**(4): p. 129-30.
18. Kinnunen, T., et al., *Heparan 2-O-sulfotransferase, hst-2, is essential for normal cell migration in Caenorhabditis elegans.* Proceedings of the National Academy of Sciences of the United States of America, 2005. **102**(5): p. 1507-12.
19. Rong, J., et al., *Substrate specificity of the heparan sulfate hexuronic acid 2-O-sulfotransferase.* Biochemistry, 2001. **40**(18): p. 5548-55.
20. Liu, C., et al., *Molecular mechanism of substrate specificity for heparan sulfate 2-O-sulfotransferase.* The Journal of biological chemistry, 2014. **289**(19): p. 13407-18.
21. Liu, J., et al., *Understanding the substrate specificity of the heparan sulfate sulfotransferases by an integrated biosynthetic and crystallographic approach.* Current opinion in structural biology, 2012. **22**(5): p. 550-7.

22. Xu, D., et al., *Mutational study of heparan sulfate 2-O-sulfotransferase and chondroitin sulfate 2-O-sulfotransferase.* The Journal of biological chemistry, 2007. **282**(11): p. 8356-67.
23. Lamanna, W.C., et al., *Sulf loss influences N-, 2-O-, and 6-O-sulfation of multiple heparan sulfate proteoglycans and modulates fibroblast growth factor signaling.* The Journal of biological chemistry, 2008. **283**(41): p. 27724-35.
24. Merry, C.L., et al., *The molecular phenotype of heparan sulfate in the Hs2st-/- mutant mouse.* The Journal of biological chemistry, 2001. **276**(38): p. 35429-34.
25. Wilson, V.A., J.T. Gallagher, and C.L. Merry, *Heparan sulfate 2-O-sulfotransferase (Hs2st) and mouse development.* Glycoconjugate journal, 2002. **19**(4-5): p. 347-54.
26. Merry, C.L. and V.A. Wilson, *Role of heparan sulfate-2-O-sulfotransferase in the mouse.* Biochimica et biophysica acta, 2002. **1573**(3): p. 319-27.
27. Esko, J.D., C. Bertozzi, and R.L. Schnaar, *Chemical Tools for Inhibiting Glycosylation*, in *Essentials of Glycobiology*, rd, et al., Editors. 2015: Cold Spring Harbor (NY). p. 701-712.
28. Bethea, H.N., et al., *Redirecting the substrate specificity of heparan sulfate 2-O-sulfotransferase by structurally guided mutagenesis.* Proceedings of the National Academy of Sciences of the United States of America, 2008. **105**(48): p. 18724-9.
29. Madhusudan, et al., *cAMP-dependent protein kinase: crystallographic insights into substrate recognition and phosphotransfer.* Protein science : a publication of the Protein Society, 1994. **3**(2): p. 176-87.
30. Teramoto, T., et al., *Crystal structure of human tyrosylprotein sulfotransferase-2 reveals the mechanism of protein tyrosine sulfation reaction.* Nature communications, 2013. **4**: p. 1572.
31. Cohen, P., *Protein kinases--the major drug targets of the twenty-first century?* Nature reviews. Drug discovery, 2002. **1**(4): p. 309-15.
32. Zhang, J., P.L. Yang, and N.S. Gray, *Targeting cancer with small molecule kinase inhibitors.* Nature reviews. Cancer, 2009. **9**(1): p. 28-39.
33. Ferguson, F.M. and N.S. Gray, *Kinase inhibitors: the road ahead.* Nature reviews. Drug discovery, 2018.
34. Drewry, D.H., et al., *Progress towards a public chemogenomic set for protein kinases and a call for contributions.* PloS one, 2017. **12**(8): p. e0181585.
35. Armstrong, J.I., et al., *Discovery of Carbohydrate Sulfotransferase Inhibitors from a Kinase-Directed Library.* Angewandte Chemie, 2000. **39**(7): p. 1303-1306.
36. Chapman, E., et al., *A potent and highly selective sulfotransferase inhibitor.* Journal of the American Chemical Society, 2002. **124**(49): p. 14524-5.
37. Armstrong, J.I., D.E. Verdugo, and C.R. Bertozzi, *Synthesis of a bisubstrate analogue targeting estrogen sulfotransferase.* The Journal of organic chemistry, 2003. **68**(1): p. 170-3.
38. Verdugo, D.E., et al., *Discovery of estrogen sulfotransferase inhibitors from a purine library screen.* Journal of medicinal chemistry, 2001. **44**(17): p. 2683-6.
39. Armstrong, J.I., et al., *A library approach to the generation of bisubstrate analogue sulfotransferase inhibitors.* Organic letters, 2001. **3**(17): p. 2657-60.
40. Baeuerle, P.A. and W.B. Huttner, *Chlorate--a potent inhibitor of protein sulfation in intact cells.* Biochemical and biophysical research communications, 1986. **141**(2): p. 870-7.
41. Bourdineaud, J.P., et al., *Enzymatic radiolabelling to a high specific activity of legume lipo-oligosaccharidic nodulation factors from Rhizobium meliloti.* The Biochemical journal, 1995. **306 (Pt 1)**: p. 259-64.
42. Verdugo, D.E. and C.R. Bertozzi, *A 96-well dot-blot assay for carbohydrate sulfotransferases.* Analytical biochemistry, 2002. **307**(2): p. 330-6.
43. Mohanty, S., et al., *Hydrophobic Core Variations Provide a Structural Framework for Tyrosine Kinase Evolution and Functional Specialization.* PLoS genetics, 2016. **12**(2): p. e1005885.
44. Rudolf, A.F., et al., *A comparison of protein kinases inhibitor screening methods using both enzymatic activity and binding affinity determination.* PloS one, 2014. **9**(6): p. e98800.
45. Linhardt, R.J., et al., *Structure and activity of a unique heparin-derived hexasaccharide.* The Journal of biological chemistry, 1986. **261**(31): p. 14448-54.
46. Yates, E.A., et al., *1H and 13C NMR spectral assignments of the major sequences of twelve systematically modified heparin derivatives.* Carbohydrate research, 1996. **294**: p. 15-27.

47. Byrne, D.P., et al., *cAMP-dependent protein kinase (PKA) complexes probed by complementary differential scanning fluorimetry and ion mobility-mass spectrometry.* The Biochemical journal, 2016. **473**(19): p. 3159-75.
48. Xu, R., et al., *Diversification of the structural determinants of fibroblast growth factor-heparin interactions: implications for binding specificity.* The Journal of biological chemistry, 2012. **287**(47): p. 40061-73.
49. Blackwell, L.J., et al., *High-throughput screening of the cyclic AMP-dependent protein kinase (PKA) using the caliper microfluidic platform.* Methods in molecular biology, 2009. **565**: p. 225-37.
50. Huynh, M.B., et al., *Age-related changes in rat myocardium involve altered capacities of glycosaminoglycans to potentiate growth factor functions and heparan sulfate-altered sulfation.* The Journal of biological chemistry, 2012. **287**(14): p. 11363-73.
51. Elkins, J.M., et al., *Comprehensive characterization of the Published Kinase Inhibitor Set.* Nature biotechnology, 2016. **34**(1): p. 95-103.
52. Jones, G., et al., *Development and validation of a genetic algorithm for flexible docking.* Journal of molecular biology, 1997. **267**(3): p. 727-48.
53. Korb, O., T. Stutzle, and T.E. Exner, *Empirical scoring functions for advanced protein-ligand docking with PLANTS.* Journal of chemical information and modeling, 2009. **49**(1): p. 84-96.
54. Dodson, C.A., et al., *A kinetic test characterizes kinase intramolecular and intermolecular autophosphorylation mechanisms.* Science signaling, 2013. **6**(282): p. ra54.
55. McSkimming, D.I., et al., *KinView: a visual comparative sequence analysis tool for integrated kinome research.* Molecular bioSystems, 2016. **12**(12): p. 3651-3665.
56. Caron, D., et al., *Mitotic phosphotyrosine network analysis reveals that tyrosine phosphorylation regulates Polo-like kinase 1 (PLK1).* Science signaling, 2016. **9**(458): p. rs14.
57. Zhou, W., et al., *A fluorescence-based high-throughput assay to identify inhibitors of tyrosylprotein sulfotransferase activity.* Biochemical and biophysical research communications, 2017. **482**(4): p. 1207-1212.
58. Davies, S.P., et al., *Specificity and mechanism of action of some commonly used protein kinase inhibitors.* The Biochemical journal, 2000. **351**(Pt 1): p. 95-105.
59. Sun, C., et al., *HaloTag is an effective expression and solubilisation fusion partner for a range of fibroblast growth factors.* PeerJ, 2015. **3**: p. e1060.
60. Bailey, F.P., et al., *The Tribbles 2 (TRB2) pseudokinase binds to ATP and autophosphorylates in a metal-independent manner.* The Biochemical journal, 2015. **467**(1): p. 47-62.
61. Murphy, J.M., et al., *A robust methodology to subclassify pseudokinases based on their nucleotide-binding properties.* The Biochemical journal, 2014. **457**(2): p. 323-34.
62. Milani, M., et al., *DRP-1 is required for BH3 mimetic-mediated mitochondrial fragmentation and apoptosis.* Cell death & disease, 2017. **8**(1): p. e2552.
63. Hay, D.A., et al., *Discovery and optimization of small-molecule ligands for the CBP/p300 bromodomains.* Journal of the American Chemical Society, 2014. **136**(26): p. 9308-19.
64. Niehrs, C., et al., *Analysis of the substrate specificity of tyrosylprotein sulfotransferase using synthetic peptides.* The Journal of biological chemistry, 1990. **265**(15): p. 8525-32.
65. Lee, R.W. and W.B. Huttner, *(Glu62, Ala30, Tyr8)n serves as high-affinity substrate for tyrosylprotein sulfotransferase: a Golgi enzyme.* Proceedings of the National Academy of Sciences of the United States of America, 1985. **82**(18): p. 6143-7.
66. Rudd, T.R. and E.A. Yates, *A highly efficient tree structure for the biosynthesis of heparan sulfate accounts for the commonly observed disaccharides and suggests a mechanism for domain synthesis.* Molecular bioSystems, 2012. **8**(5): p. 1499-506.
67. Yoshida-Moriguchi, T., et al., *SGK196 is a glycosylation-specific O-mannose kinase required for dystroglycan function.* Science, 2013. **341**(6148): p. 896-9.
68. Zhu, Q., et al., *Structure of protein O-mannose kinase reveals a unique active site architecture.* eLife, 2016. **5**.
69. McGeary, R.P., et al., *Suramin: clinical uses and structure-activity relationships.* Mini reviews in medicinal chemistry, 2008. **8**(13): p. 1384-94.

70. Givens, J.F. and K.F. Manly, *Inhibition of RNA-directed DNA polymerase by aurintricarboxylic acid.* Nucleic acids research, 1976. **3**(2): p. 405-18.
71. Gschwendt, M., et al., *Rottlerin, a novel protein kinase inhibitor.* Biochemical and biophysical research communications, 1994. **199**(1): p. 93-8.
72. Lackey, K., et al., *The discovery of potent cRaf1 kinase inhibitors.* Bioorganic & medicinal chemistry letters, 2000. **10**(3): p. 223-6.
73. Scutt, P.J., et al., *Discovery and exploitation of inhibitor-resistant aurora and polo kinase mutants for the analysis of mitotic networks.* The Journal of biological chemistry, 2009. **284**(23): p. 15880-93.
74. Sloane, D.A., et al., *Drug-resistant aurora A mutants for cellular target validation of the small molecule kinase inhibitors MLN8054 and MLN8237.* ACS chemical biology, 2010. **5**(6): p. 563-76.
75. Bailey, F.P., V.I. Andreev, and P.A. Eyers, *The resistance tetrad: amino acid hotspots for kinome-wide exploitation of drug-resistant protein kinase alleles.* Methods in enzymology, 2014. **548**: p. 117-46.
76. Xu, D., et al., *Engineering sulfotransferases to modify heparan sulfate.* Nature chemical biology, 2008. **4**(3): p. 200-2.
77. Wu, Z.S., et al., *Suramin blocks interaction between human FGF1 and FGFR2 D2 domain and reduces downstream signaling activity.* Biochemical and biophysical research communications, 2016. **477**(4): p. 861-867.
78. Antolin, A.A., et al., *Objective, Quantitative, Data-Driven Assessment of Chemical Probes.* Cell chemical biology, 2018. **25**(2): p. 194-205 e5.
79. Cohen, P., *Guidelines for the effective use of chemical inhibitors of protein function to understand their roles in cell regulation.* The Biochemical journal, 2009. **425**(1): p. 53-4.

Figure 1

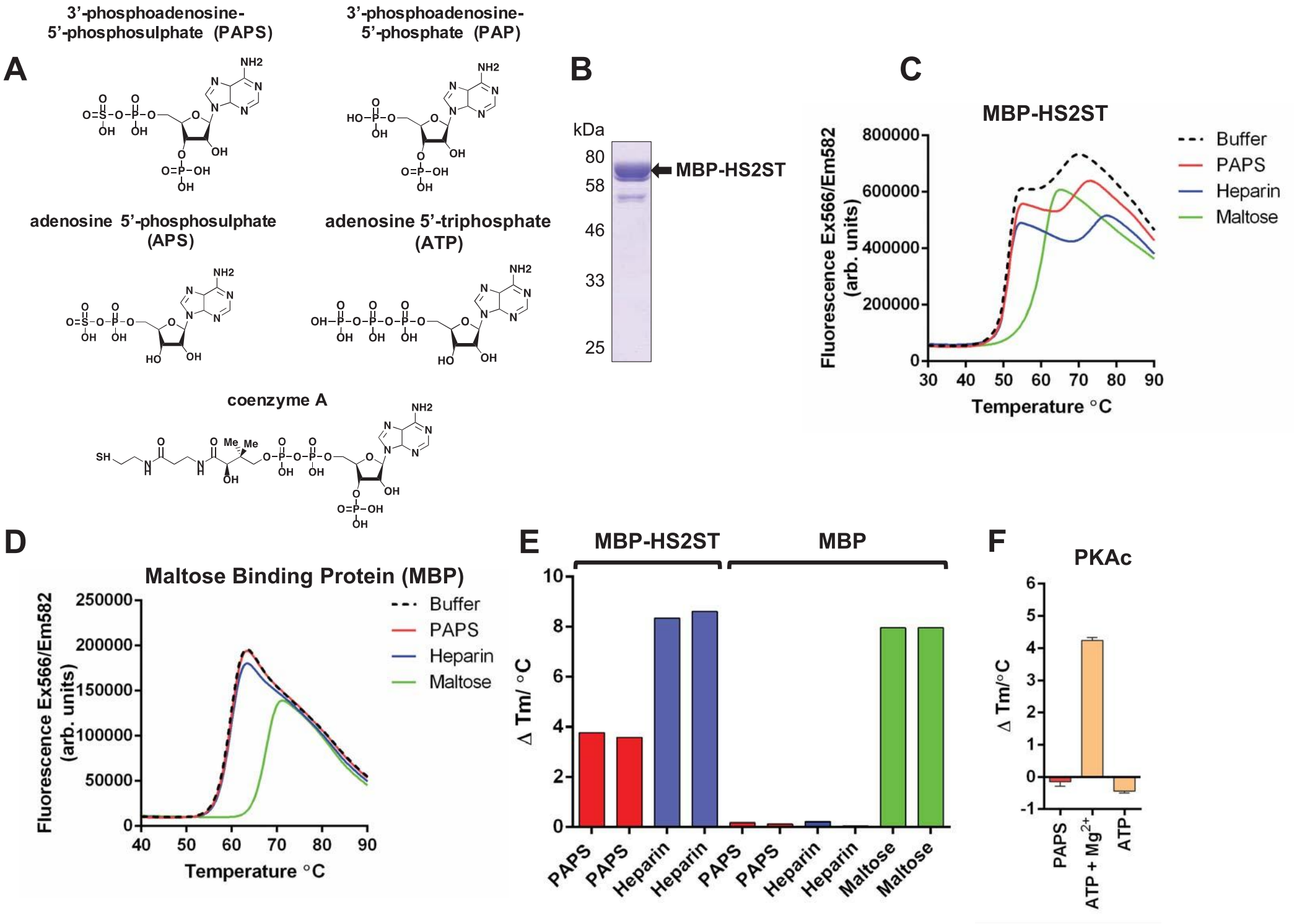
A
3'-phosphoadenosine-5'-phosphosulphate (PAPS)
3'-phosphoadenosine-5'-phosphate (PAP)
adenosine 5'-phosphosulphate (APS)
adenosine 5'-triphosphate (ATP)
coenzyme A
B
kDa
80
58
46
33
25
MBP-HS2ST
C
MBP-HS2ST
Fluorescence Ex566/Em582 (arb. units)
Temperature °C
Buffer
PAPS
Heparin
Maltose
D
Maltose Binding Protein (MBP)
Fluorescence Ex566/Em582 (arb. units)
Temperature °C
Buffer
PAPS
Heparin
Maltose
E
MBP-HS2ST
MBP
Δ Tm/ °C
PAPS
PAPS
Heparin
Heparin
PAPS
PAPS
Heparin
Heparin
Maltose
Maltose
F
PKAc
Δ Tm/°C
PAPS
ATP + Mg2+
ATP

Figure 2

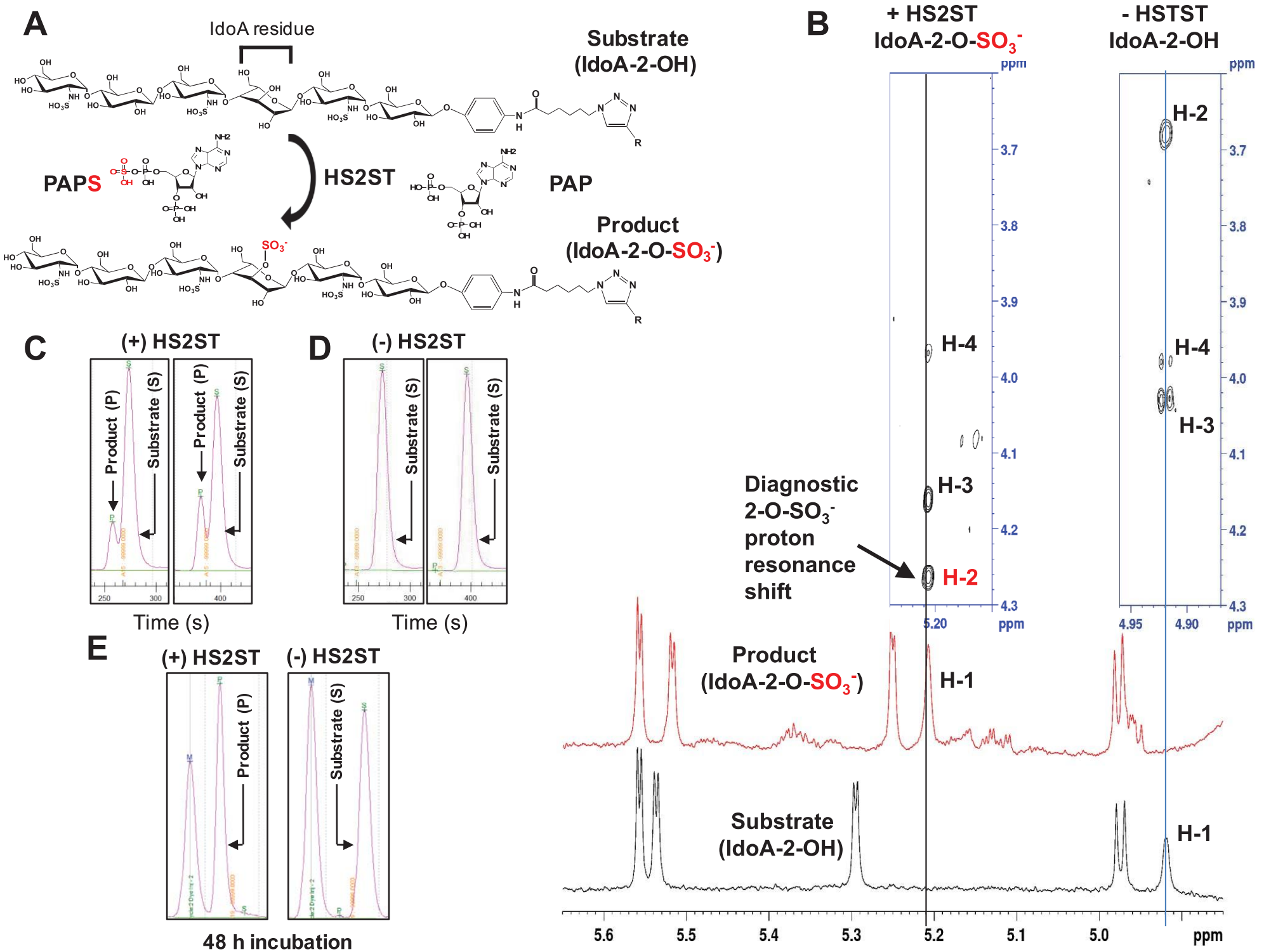
A
IdoA residue
Substrate
(IdoA-2-OH)
PAPS
HS2ST
PAP
Product
(IdoA-2-O-SO3-)
B
+ HS2ST
IdoA-2-O-SO3-
- HSTST
IdoA-2-OH
ppm
H-2
H-4
H-3
H-2
H-4
H-3
Diagnostic
2-O-SO3-
proton
resonance
shift
5.20
4.95
4.90
Product
(IdoA-2-O-SO3-)
H-1
Substrate
(IdoA-2-OH)
H-1
5.6
5.5
5.4
5.3
5.2
5.1
5.0
ppm
C
(+) HS2ST
Product (P)
Substrate (S)
Product (P)
Substrate (S)
Time (s)
D
(-) HS2ST
Substrate (S)
Substrate (S)
Time (s)
E
(+) HS2ST
(-) HS2ST
Product (P)
Substrate (S)
48 h incubation

Figure 2 continued

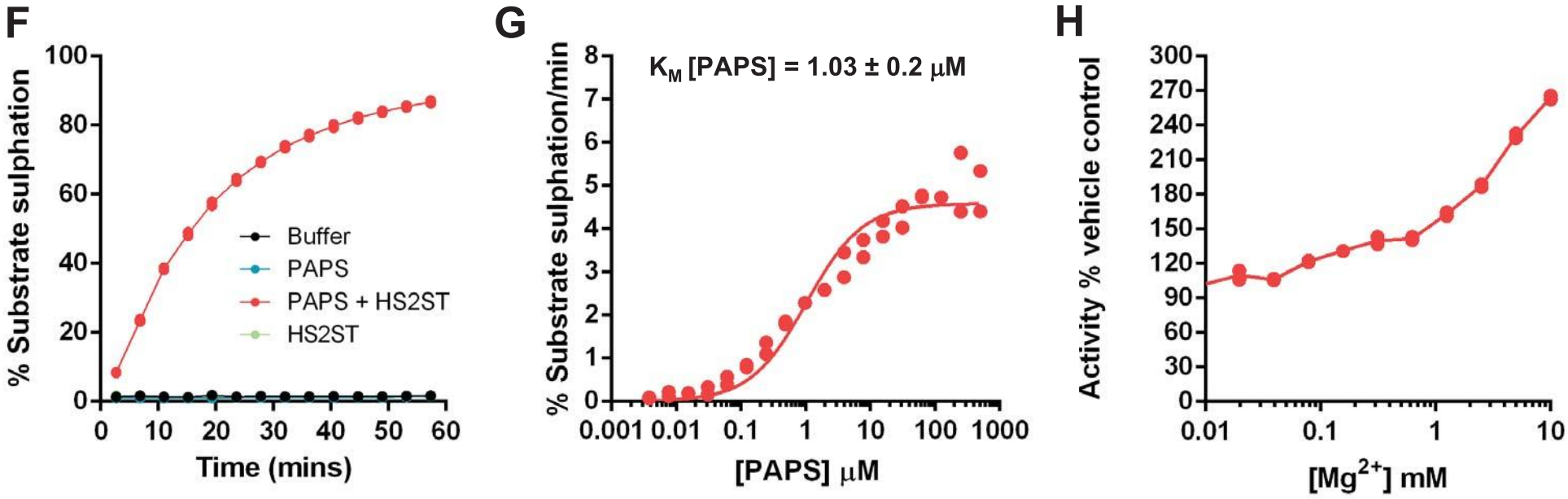

Figure 3

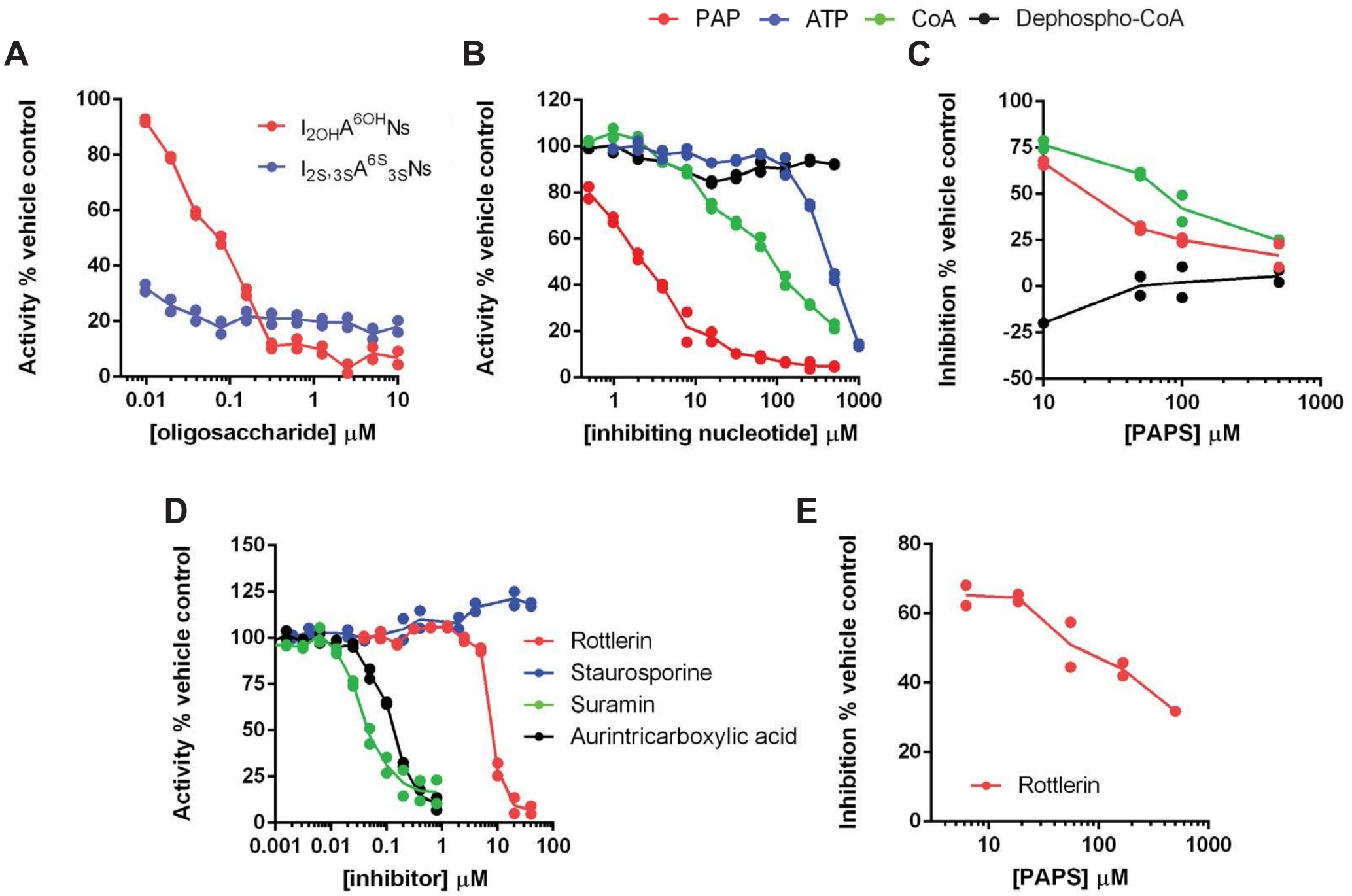
A
B
C
D
E
PAP
ATP
CoA
Dephospho-CoA
Activity % vehicle control
[oligosaccharide] μM
[inhibiting nucleotide] μM
Inhibition % vehicle control
[PAPS] μM
Rottlerin
Staurosporine
Suramin
Aurintricarboxylic acid
[inhibitor] μM

Figure 4

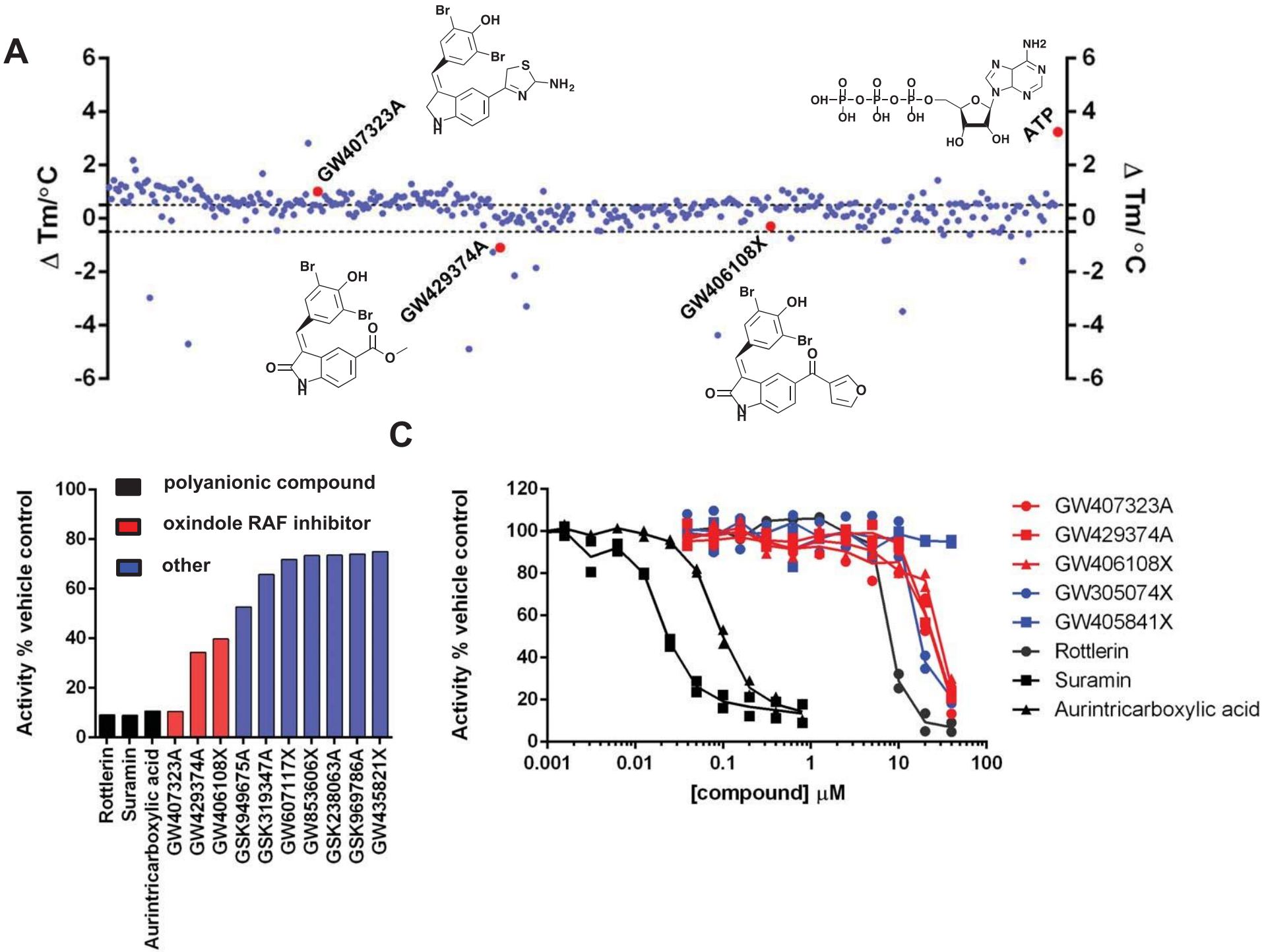
A
Δ Tm/°C
Δ Tm/ °C
GW407323A
GW429374A
GW406108X
ATP
B
Activity % vehicle control
polyanionic compound
oxindole RAF inhibitor
other
Rottlerin
Suramin
Aurintricarboxylic acid
GW407323A
GW429374A
GW406108X
GSK949675A
GSK319347A
GW607117X
GW853606X
GSK238063A
GSK969786A
GW435821X
C
Activity % vehicle control
[compound] μM
GW407323A
GW429374A
GW406108X
GW305074X
GW405841X
Rottlerin
Suramin
Aurintricarboxylic acid

Figure 5

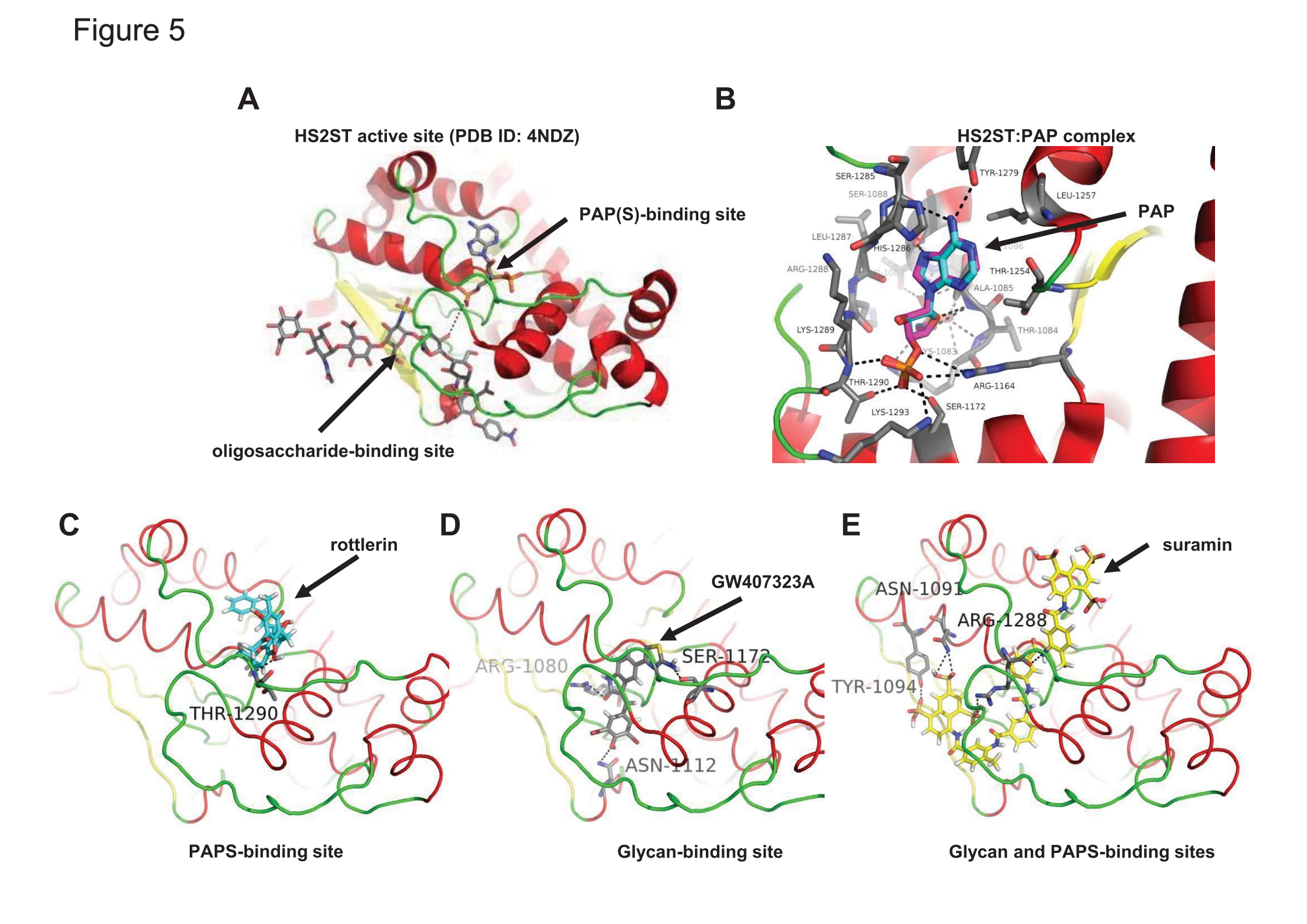
A
HS2ST active site (PDB ID: 4NDZ)
PAP(S)-binding site
oligosaccharide-binding site
B
HS2ST:PAP complex
PAP
SER-1285
SER-1088
TYR-1279
LEU-1257
LEU-1287
HIS-1286
ARG-1288
THR-1254
ALA-1085
LYS-1289
THR-1084
LYS-1083
THR-1290
ARG-1164
SER-1172
LYS-1293
C
rottlerin
THR-1290
PAPS-binding site
D
GW407323A
ARG-1080
SER-1172
ASN-1112
Glycan-binding site
E
suramin
ASN-1091
ARG-1288
TYR-1094
Glycan and PAPS-binding sites

Supplementary Figure 1

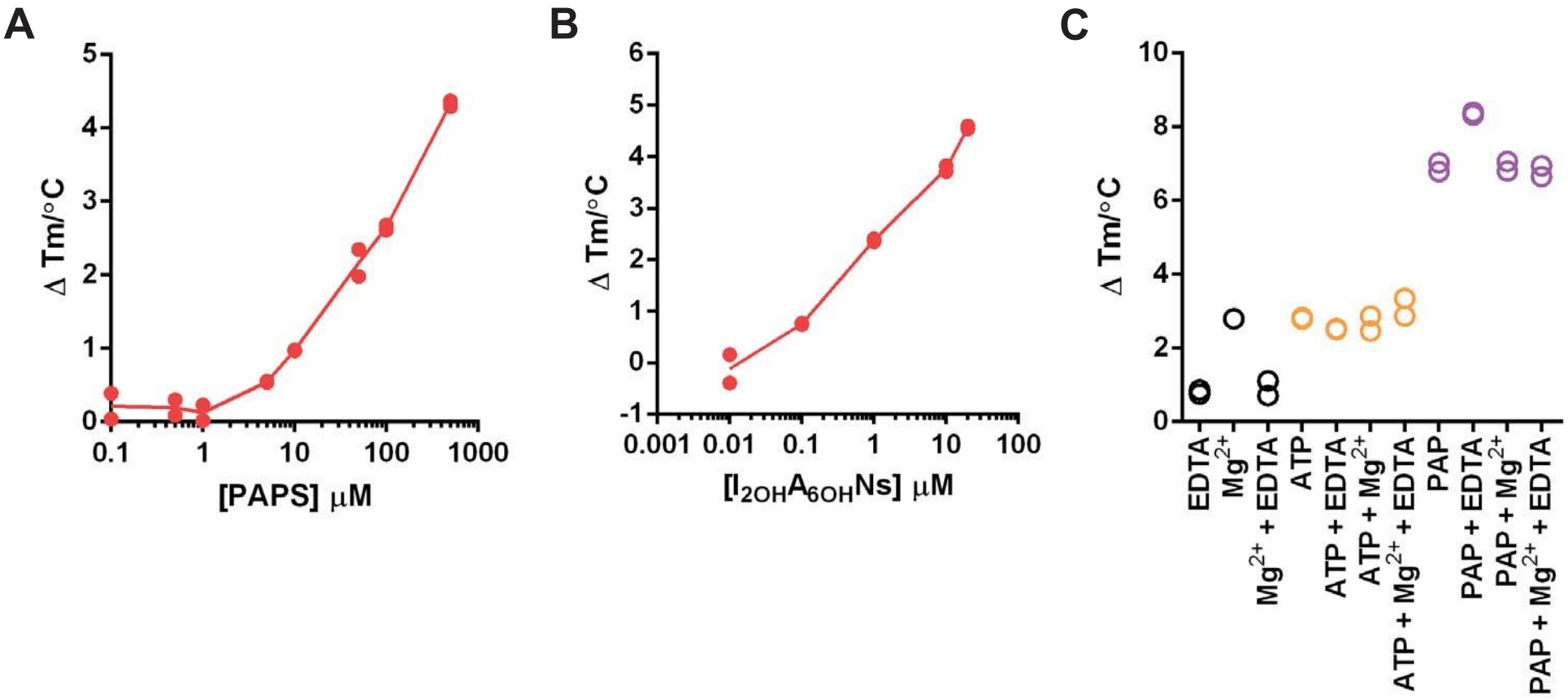

Supplementary Figure 2

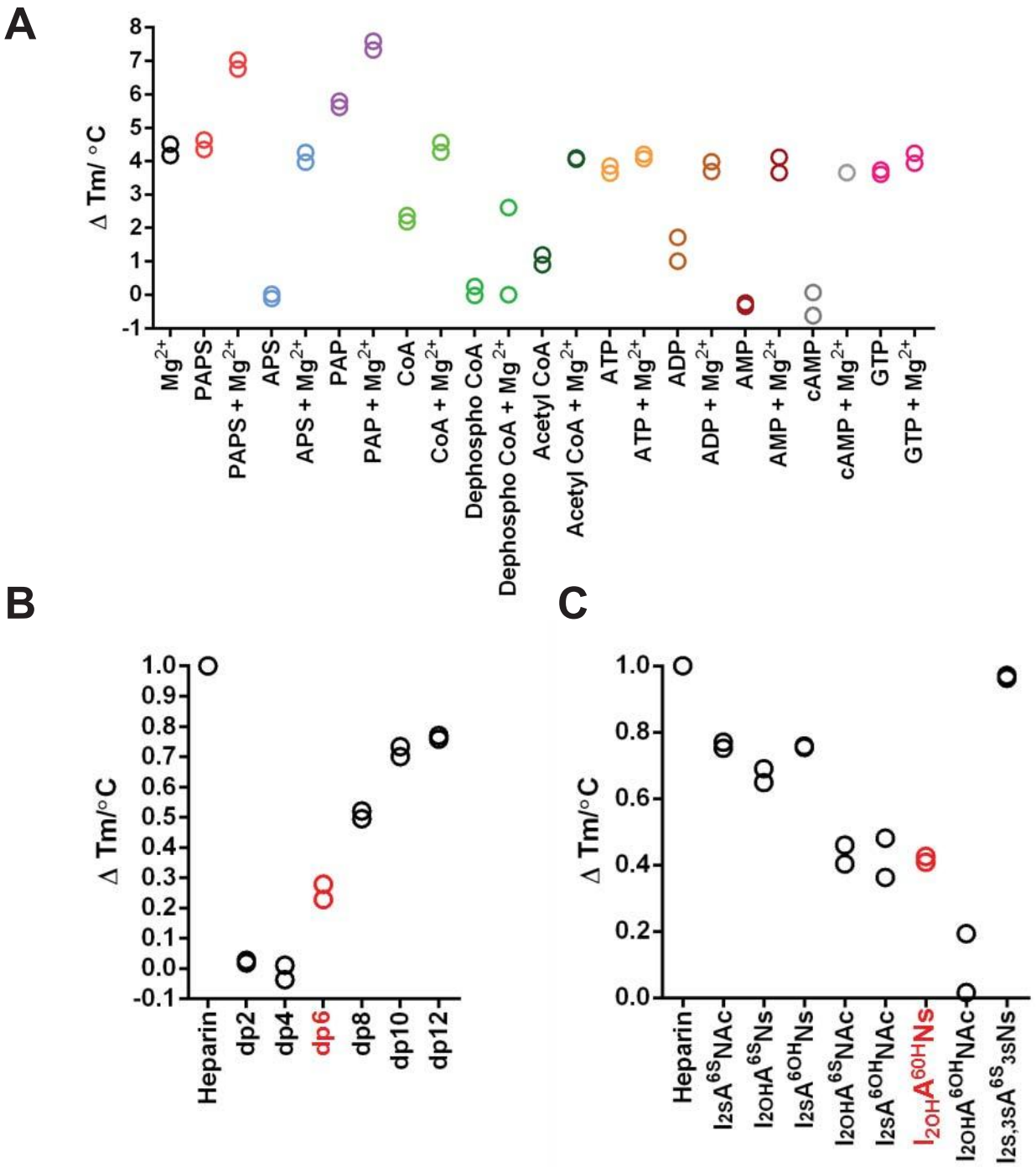

Supplementary Figure 3

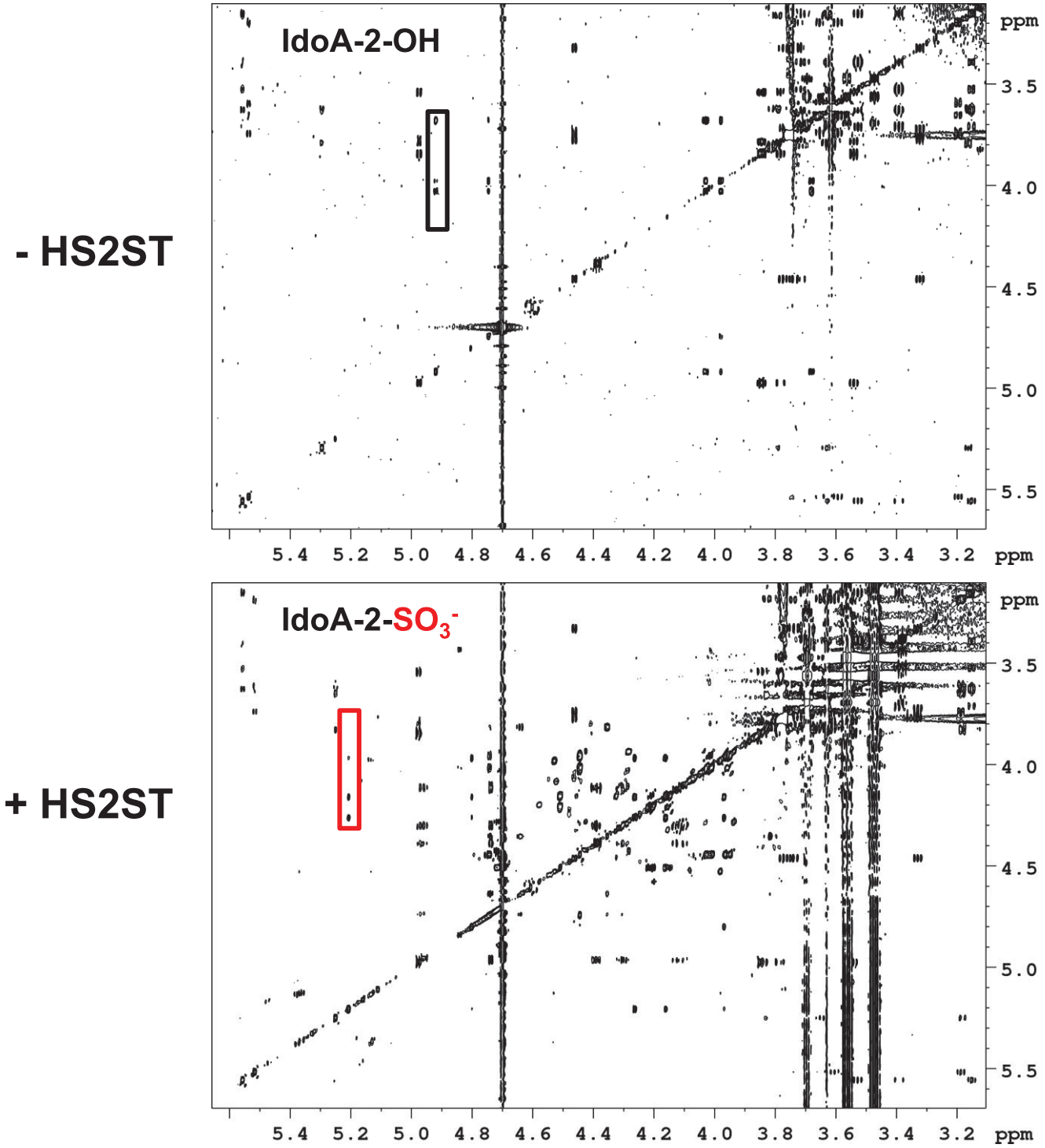

Supplementary Figure 4

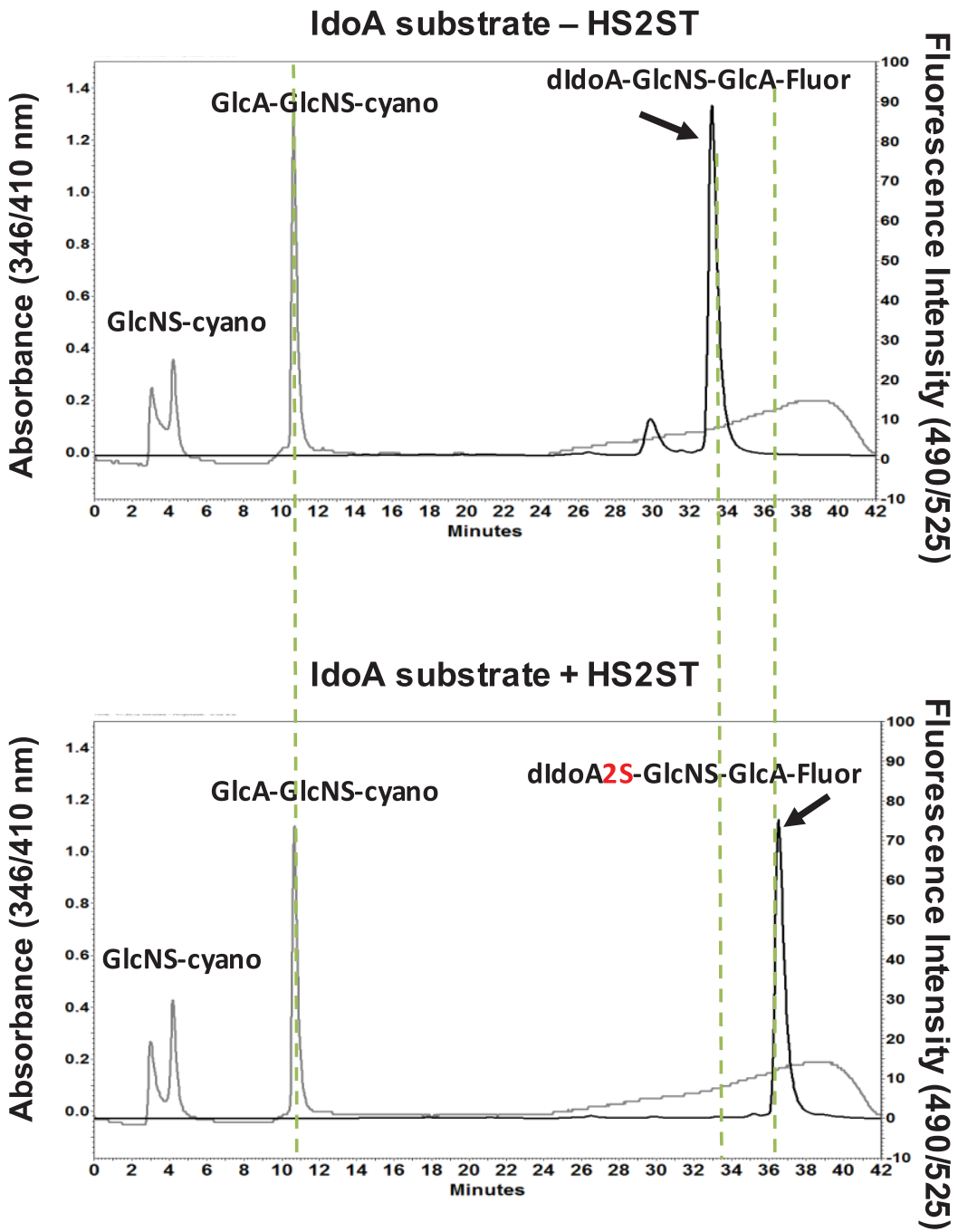

Supplementary Figure 5

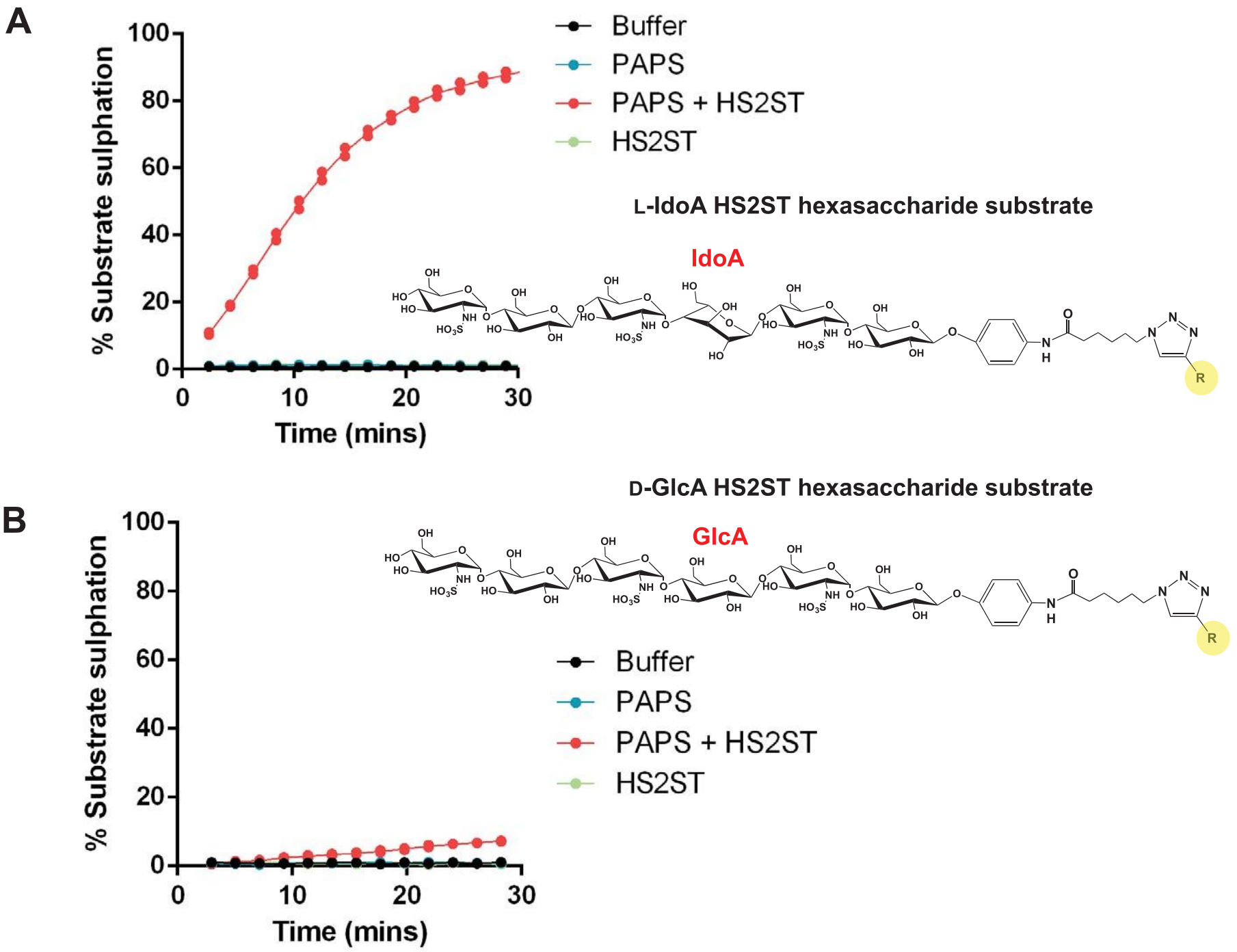

Supplementary Figure 6

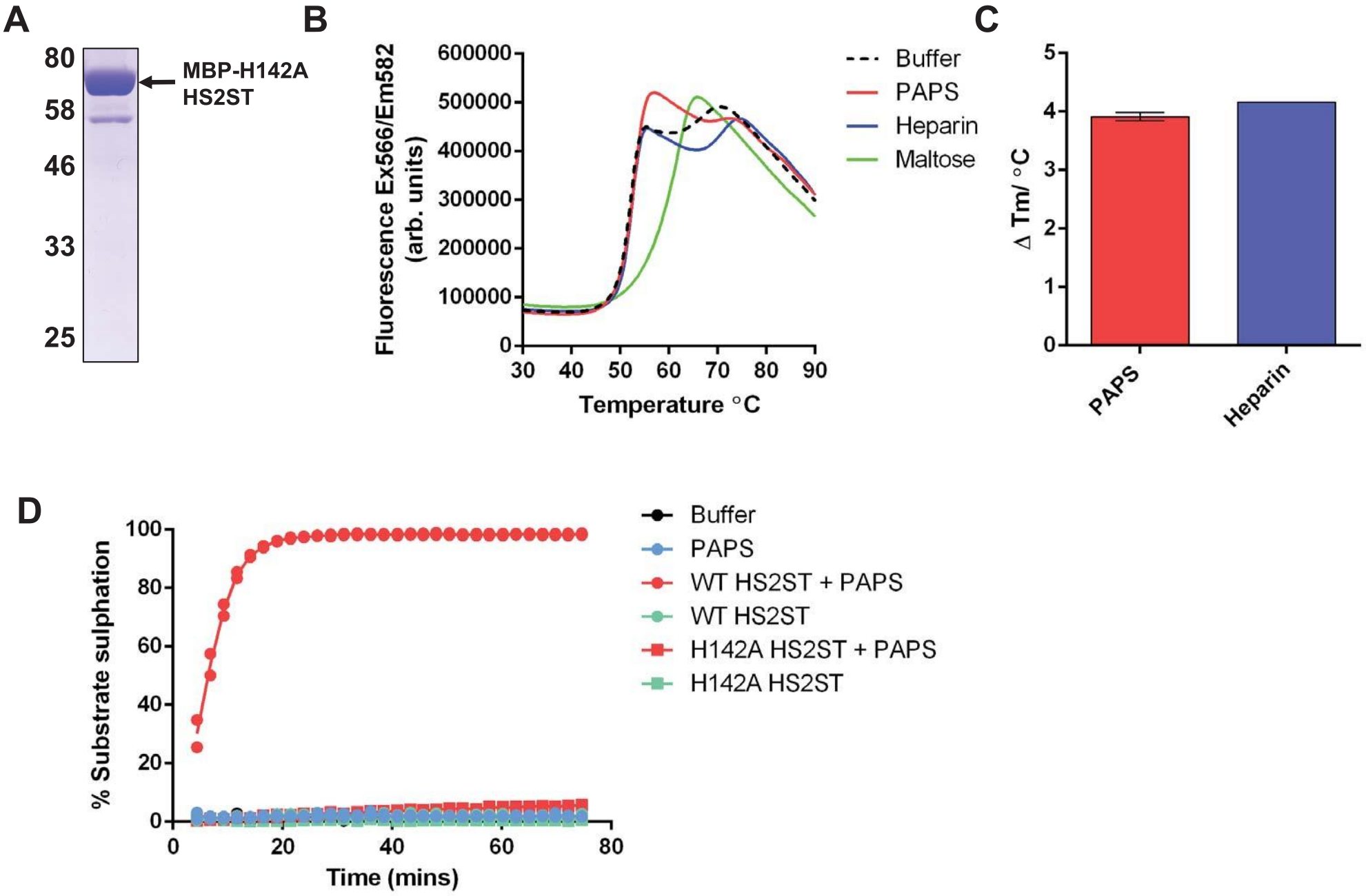

Supplementary Figure 7

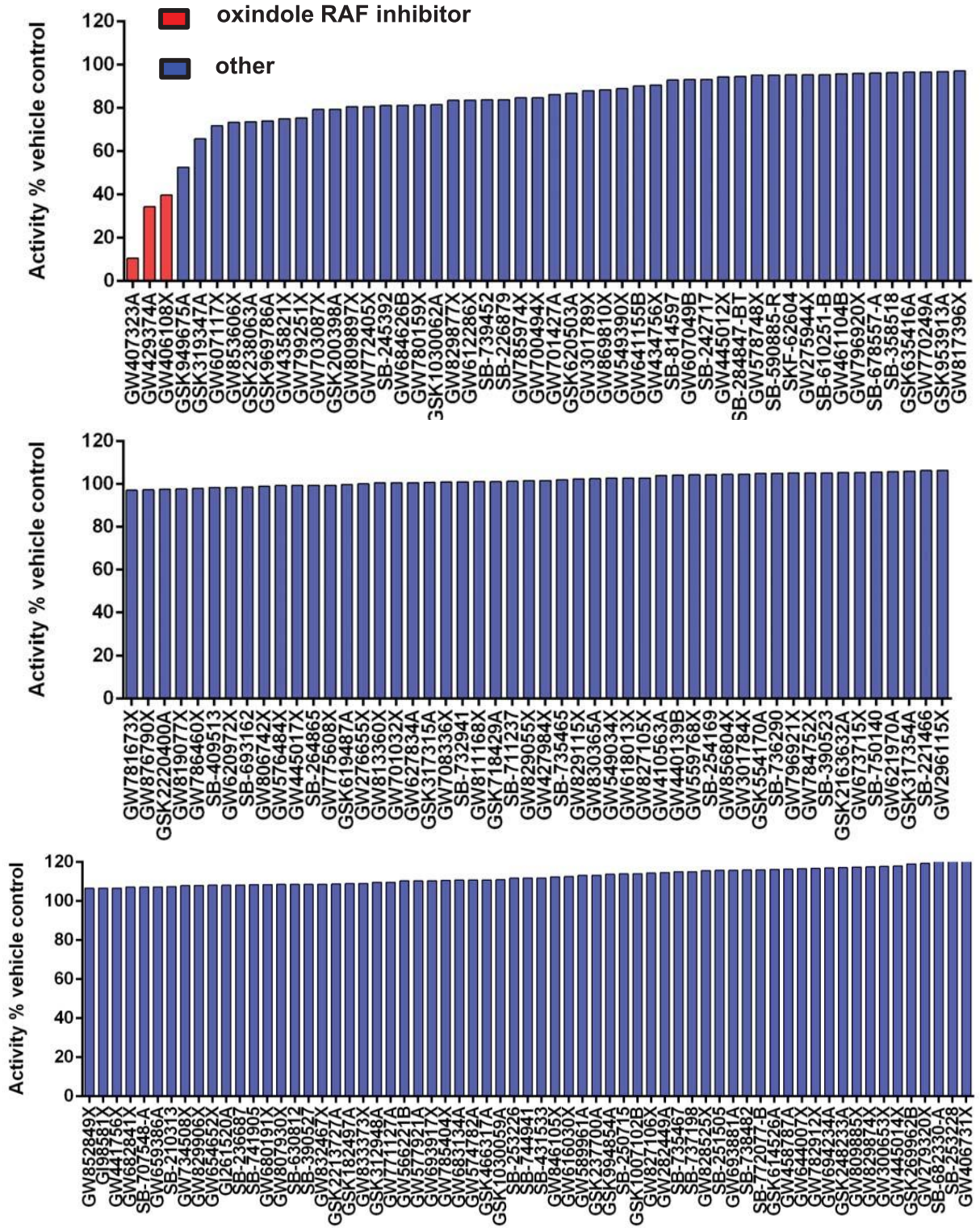

Supplementary Figure 8

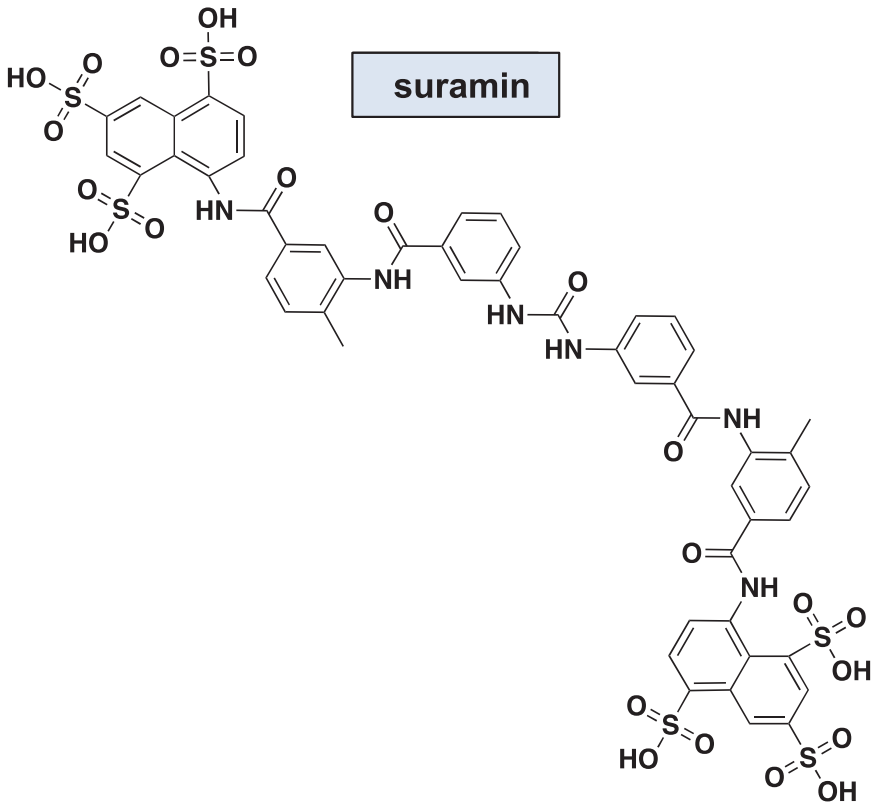

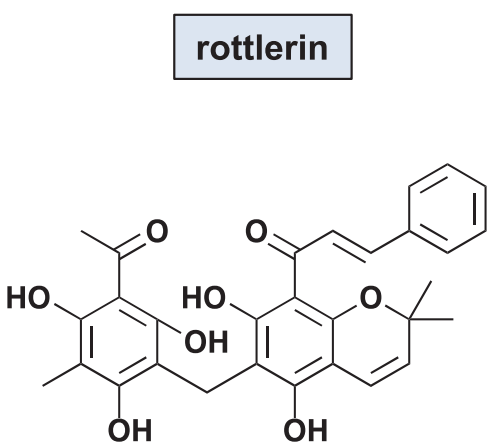

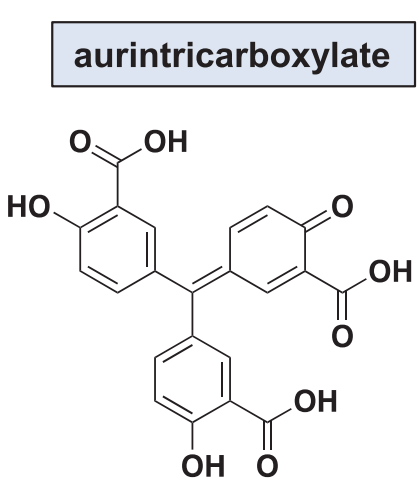

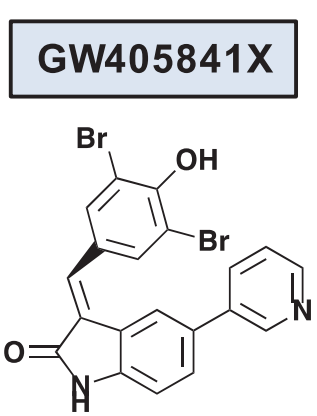

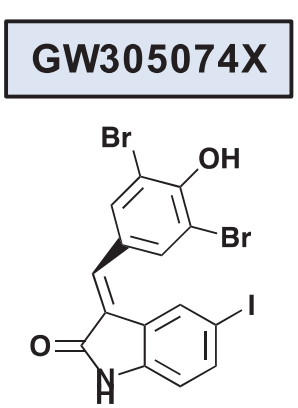

Supplementary Figure 9